

# Study of the $\overline{B}_q^* \rightarrow DM$ decays with perturbative QCD approach

Junfeng Sun, Jie Gao, Yueling Yang, Qin Chang, Na Wang, and Gongru Lu

*Institute of Particle and Nuclear Physics,*

*Henan Normal University, Xinxiang 453007, China*

Jinshu Huang

*College of Physics and Electronic Engineering,*

*Nanyang Normal University, Nanyang 473061, China*

## Abstract

The  $\overline{B}_q^* \rightarrow DP, DV$  weak decays are studied with the perturbative QCD approach, where  $q = u, d$  and  $s$ ;  $P$  and  $V$  denote the ground  $SU(3)$  pseudoscalar and vector meson nonet. It is found that the branching ratios for the color-allowed  $\overline{B}_q^* \rightarrow D_q \rho^-$  decays can reach up to  $10^{-9}$  or more, and should be promisingly measurable at the running LHC and forthcoming SuperKEKB experiments in the near future.

## I. INTRODUCTION

In accordance with the conventional quark model assignments, the ground spin-singlet pseudoscalar  $B_q$  mesons and spin-triplet vector  $B_q^*$  mesons have the same flavor components, and consist of one valence heavy antiquark  $\bar{b}$  and one light quark  $q$ , i.e.,  $\bar{b}q$ , with  $q = u, d, s$  [1]. With the two  $e^+e^-$   $B$ -factory BaBar and Belle experiments, there is a combined data sample of over  $1\text{ ab}^{-1}$  at the  $\Upsilon(4S)$  resonance. The  $B_{u,d}$  meson weak decay modes with branching ratio of over  $10^{-6}$  have been well measured [2]. The  $B_s$  meson, which can be produced in hadron collisions or at/over the resonance  $\Upsilon(5S)$  in  $e^+e^-$  collisions<sup>1</sup>, is being carefully scrutinized. However, the study of the  $B_q^*$  mesons has not actually attracted much attention yet, subject to the relatively inadequate statistics. Because the mass of the  $B_q^*$  mesons is a bit larger than that of the  $B_q$  mesons, the  $B_q^*$  meson should be produced at the relatively higher energy rather than at the resonance  $\Upsilon(4S)$  in  $e^+e^-$  collisions. With the high luminosities and large production cross section at the running LHC, the forthcoming SuperKEKB and future *Super proton proton Collider* (SppC, which is still in the preliminary discussion and research stage up to now), more and more  $B_q^*$  mesons will be accumulated in the future, which makes the  $B_q^*$  mesons another research laboratory for testing the Cabibbo-Kobayashi-Maskawa (CKM) picture for  $CP$ -violating phenomena, examining our comprehension of the underlying dynamical mechanism for the weak decays of the heavy flavor hadrons.

Having the same valence quark components and approximately an equal mass, both the  $B_q^*$  and  $B_q$  mesons can decay via weak interactions into the same final states. On the one hand, the  $B_q^*$  and  $B_q$  meson weak decays would provide each other with a spurious background; on the other hand, the interplay between the  $B_q^*$  and  $B_q$  weak decays could offer some potential useful information to constrain parameters within the standard model, and might shed some fresh light on various intriguing puzzles in the  $B_q$  meson decays. The  $B_q$  meson decays are well described by the bottom quark decay with the light spectator quark  $q$  in the spectator model. At the quark level, most of the hadronic  $B_q$  meson decays involve the  $b \rightarrow c$  transition due to the hierarchy relation among the CKM matrix elements. As is well known, there is a more than  $3\sigma$  discrepancy between the value of  $|V_{cb}|$  obtained

---

<sup>1</sup> In hadron colliders, CDF and D0 each have accumulated about  $10\text{ fb}^{-1}$  data, and LHCb has accumulated over  $5\text{ fb}^{-1}$  data up to the year of 2016 [3]. In  $e^+e^-$  colliders, Belle has accumulated more than  $100\text{ fb}^{-1}$  data at the resonance  $\Upsilon(5S)$  [2].

from inclusive determinations,  $|V_{cb}| = (42.2 \pm 0.8) \times 10^{-3}$ , and from exclusive ones,  $|V_{cb}| = (39.2 \pm 0.7) \times 10^{-3}$  [1]. Besides the semileptonic  $\overline{B}_q^{(*)} \rightarrow D^{(*)} \ell \bar{\nu}$  decays, the nonleptonic  $\overline{B}_q^{(*)} \rightarrow DM$  decays, with  $M$  representing the ground  $SU(3)$  pseudoscalar  $P$  and the vector  $V$  meson nonet, are also induced by the  $b \rightarrow c$  transition, and hence could be used to extract/constrain the CKM matrix element  $|V_{cb}|$ .

From the dynamical point of view, the phenomenological models used for the  $\overline{B}_q \rightarrow DM$  decays might, in principle, be extended and applied to the  $\overline{B}_q^* \rightarrow DM$  decays. The practical applicability and reliability of these models could be reevaluated with the  $\overline{B}_q^* \rightarrow DM$  decays. Recently, some attractive QCD-inspired methods, such as the perturbative QCD (pQCD) approach [4–11], the QCD factorization (QCDF) approach [12–19], soft and collinear effective theory [20–27] and so on, have been developed vigorously and employed widely to explain measurements on the  $B_q$  meson decays. The  $\overline{B}_q \rightarrow DM$  decays have been studied with the QCDF [13, 28] and pQCD [29, 30] approaches, but there are few research works on the  $B_q^*$  meson weak decays. Recently, the  $\overline{B}_q^* \rightarrow D_q V$  decays have been investigated with the QCDF approach [31], and it is shown that the  $\overline{B}_q^{*0} \rightarrow D_q^+ \rho^-$  decays with branching ratios of  $\mathcal{O}(10^{-8})$  might be accessible to the existing and future heavy flavor experiments. In this paper, we will give a comprehensive investigation into the two-body nonleptonic  $\overline{B}_q^* \rightarrow DM$  decays with the pQCD approach in order to provide the future experimental research with an available reference.

As is well known, the  $B_q^*$  meson decays are dominated by the electromagnetic interactions rather than the weak interactions, which differs significantly from the  $B_q$  meson decays. One can easily expect that the branching ratios for the  $\overline{B}_q^* \rightarrow DM$  weak decays should be very small due to the short electromagnetic lifetimes of the  $B_q^*$  mesons [32], although these processes are favored by the CKM matrix element  $|V_{cb}|$ . Of course, an abnormal large branching ratio might be a possible hint of new physics beyond the standard model. There is still no experimental report on the  $\overline{B}_q^* \rightarrow DM$  weak decays so far. Furthermore, the  $\overline{B}_q^* \rightarrow DM$  weak decays offer the unique opportunity of observing the weak decay of a vector meson, where polarization effects could be explored.

This paper is organized as follows. In section II, we present the theoretical framework, the conventions and notations, together with amplitudes for the  $\overline{B}_q^* \rightarrow DM$  decays. Section III is devoted to the numerical results and discussion. The final section is a summary.

## II. THEORETICAL FRAMEWORK

### A. The effective Hamiltonian

As is well known, the weak decays of the  $B_q^{(*)}$  mesons inevitably involve multiple length scales, including the mass of  $m_W$  for the virtual gauge boson  $W$ , the mass of  $m_b$  for the decaying bottom quark, the infrared confinement scale  $\Lambda_{\text{QCD}}$  of the strong interactions, and  $m_W \gg m_b \gg \Lambda_{\text{QCD}}$ . So, one usually has to resort to the effective theory approximation scheme. With the operator product expansion and the renormalization group (RG) method, the effective Hamiltonian for the  $\overline{B}_q^* \rightarrow DM$  decays can be written as [33],

$$\mathcal{H}_{\text{eff}} = \frac{G_F}{\sqrt{2}} \sum_{q'=d,s} V_{cb} V_{uq'}^* \left\{ C_1(\mu) Q_1(\mu) + C_2(\mu) Q_2(\mu) \right\} + \text{h.c.}, \quad (1)$$

where  $G_F \simeq 1.166 \times 10^{-5} \text{ GeV}^{-2}$  [1] is the Fermi coupling constant.

Using the Wolfenstein parametrization, the CKM factor  $V_{cb} V_{uq'}^*$  are expressed as a series expansion of the small Wolfenstein parameter  $\lambda \approx 0.2$  [1]. Up to the order of  $\mathcal{O}(\lambda^7)$ , they can be written as follows:

$$V_{cb} V_{ud}^* = A \lambda^2 (1 - \lambda^2/2 - \lambda^4/8) + \mathcal{O}(\lambda^7), \quad (2)$$

$$V_{cb} V_{us}^* = A \lambda^3 + \mathcal{O}(\lambda^7). \quad (3)$$

It is very clearly seen that the both  $V_{cb} V_{ud}^*$  and  $V_{cb} V_{us}^*$  are real-valued, i.e., there is no weak phase difference. However, nonzero weak phase difference is necessary and indispensable for the direct  $CP$  violation. Therefore, none of direct  $CP$  violation should be expected for the  $\overline{B}_q^* \rightarrow DM$  decays.

The renormalization scale  $\mu$  separates the physical contributions into the short- and long-distance parts. The Wilson coefficients  $C_{1,2}$  summarize the physical contributions above the scale  $\mu$ . They, in principle, are calculable order by order in the strong coupling  $\alpha_s$  at the scale  $m_W$  with the ordinary perturbation theory, and then evolved with the RG equation to the characteristic scale  $\mu \sim \mathcal{O}(m_b)$  for the bottom quark decay [33]. The Wilson coefficients at the scale  $m_W$  are determined at the quark level rather than the hadron level, so they are regarded as process-independent couplings of the local operators  $Q_i$ . Their explicit analytical expressions, including the next-to-leading order corrections, have been given in Ref.[33].

The physical contributions from the scales lower than  $\mu$  are contained in the hadronic matrix elements (HME) where the local four-quark operators are sandwiched between the

initial and final hadron states. The local six-dimension operators arising from the  $W$ -boson exchange are defined as follows:

$$Q_1 = [\bar{c}_\alpha \gamma_\mu (1 - \gamma_5) b_\alpha] [\bar{q}'_\beta \gamma^\mu (1 - \gamma_5) u_\beta], \quad (4)$$

$$Q_2 = [\bar{c}_\alpha \gamma_\mu (1 - \gamma_5) b_\beta] [\bar{q}'_\beta \gamma^\mu (1 - \gamma_5) u_\alpha]. \quad (5)$$

where  $\alpha$  and  $\beta$  are color indices, i.e., the gluonic corrections are included. The operator  $Q_1$  ( $Q_2$ ) consists of two color-singlet (color-octet) currents. The operators  $Q_1$  and  $Q_2$ , called current-current operators or tree operators, have the same flavor form and a different color structure. It is obvious that the  $\bar{B}_q^* \rightarrow DM$  decays are uncontaminated by the contributions from the penguin operators, which is positive to extract the CKM matrix element  $|V_{cb}|$ .

Because of the participation of the strong interaction, especially, the long-distance effects in the conversion from the quarks of the local operators to the initial and final hadrons, barricades are still erected on the approaches of nonleptonic  $\bar{B}_q^{(*)}$  weak decays, which complicates the calculation. HME of the local operators are the most intricate part for theoretical calculation, where the perturbative and nonperturbative contributions entangle with each other. To evaluate the HME amplitudes, one usually has to resort to some plausible approximations and assumptions, which results in the model-dependence of theoretical predictions. It is obvious that a large part of the uncertainties does come from the practical treatment of HME, due to our inadequate understanding of the hadronization mechanism and the low-energy QCD behavior. For the phenomenology of the  $\bar{B}_q^* \rightarrow DM$  decays, one of the main tasks at this stage is how to effectively factorize HME of the local operators into hard and soft parts, and how to evaluate HME properly.

## B. Hadronic matrix elements

One of the phenomenological schemes for the HME calculation is the factorization approximation based on Bjorken's *a priori* color transparency hypothesis, which says that the color singlet energetic hadron would have flown rapidly away from the color fields existing in the neighborhood of the interaction point before the soft gluons are exchanged among hadrons [34]. Modeled on the amplitudes for exclusive processes with the Lepage-Brodsky approach [35], HME are usually written as the convolution integral of the hard kernels and the hadron distribution amplitudes (DAs). Hard kernels are expressed as the scattering am-

plitudes for the transition of the heavy bottom quark into light quarks. They are generally computable at the quark level with the perturbation theory as a series of expansion in the parameter  $1/m_b$  and the strong coupling constant  $\alpha_s$  in the heavy quark limit. It is assumed that the soft and nonperturbative contributions of HME could be absorbed into hadron DAs. The distribution amplitudes are functions of parton momentum fractions. They, although not calculable, are regarded as universal and can be determined by nonperturbative means or extracted from data. With the traits of universality and determinability of hadron DAs, HME have a sample structure and can be evaluated to make predictions.

Besides the factorizable contributions to HME, the nonfactorizable corrections to HME also play an important role in commenting on the experimental measurements and solving the so-called puzzles and anomalies, and hence should be carefully considered, as commonly recognized by theoretical physicists. In order to regulate the endpoint singularities which appear in the spectator scattering and annihilation amplitudes with the QCDF approach and spoil the perturbative calculation with the collinear approximation [13–17], it is suggested by the pQCD approach [4–11] that the transverse momentum of quarks should be conserved and, additionally, that a Sudakov factor should be introduced to DAs for all the participant hadrons to further suppress the long-distance and soft contributions. The basic pQCD formula for nonleptonic weak decay amplitudes could be factorized into three parts: the hard effects enclosed by the Wilson coefficients  $C_i$ , hard scattering kernels  $\mathcal{H}_i$ , and the universal wave functions  $\Phi_j$ . The general form is a multidimensional integral [4–11],

$$\mathcal{A}_i \propto \int \prod_j dx_j db_j C_i(t) \mathcal{H}_i(t_i, x_j, b_j) \Phi_j(x_j, b_j) e^{-S_j}, \quad (6)$$

where  $x_j$  is the longitudinal momentum fraction of the valence quarks.  $b_j$  is the conjugate variable of the transverse momentum  $k_{jT}$ . The scale  $t_i$  is preferably chosen to be the maximum virtuality of all the internal particles. The Sudakov factor  $e^{-S_j}$ , together with the particular scale  $t_i$ , will ensure the perturbative calculation is feasible and reliable.

### C. Kinematic variables

The  $\overline{B}_q^{(*)}$  weak decays are actually dominated by the  $b$  quark weak decay. In the heavy quark limit, the light quark originating from the heavy bottom quark decay is assumed to be energetic and race quickly away from the weak interaction point. If the velocity  $v \sim c$

(the speed of light), the light quarks move near the light-cone line. The light-cone dynamics can be used to describe the relativistic system along the light-front direction. The light-cone coordinates  $(x^+, x^-, x_\perp)$  of space-time are defined as  $x^\pm = (x^0 \pm x^3)/\sqrt{2}$  (or  $(t \pm x^3)/\sqrt{2}$ ) and  $x_\perp = x^i$  with  $i = 1$  and  $2$ .  $x^\pm = 0$  is called the light-front. The scalar product of any two four-dimensional vectors is given by  $a \cdot b = a_\mu b^\mu = a^+ b^- + a^- b^+ - a_\perp \cdot b_\perp$ . In the rest frame of the  $\overline{B}_q^*$  meson, the final  $D$  and  $M$  mesons are back-to-back. The light-cone kinematic variables are defined as follows:

$$p_{\overline{B}_q^*} = p_1 = \frac{m_1}{\sqrt{2}}(1, 1, 0), \quad (7)$$

$$p_D = p_2 = (p_2^+, p_2^-, 0), \quad (8)$$

$$p_M = p_3 = (p_3^-, p_3^+, 0), \quad (9)$$

$$k_i = x_i p_i + (0, 0, k_{iT}), \quad (10)$$

$$p_i^\pm = (E_i \pm p)/\sqrt{2}, \quad (11)$$

$$t = 2 p_1 \cdot p_2 = m_1^2 + m_2^2 - m_3^2 = 2 m_1 E_2, \quad (12)$$

$$u = 2 p_1 \cdot p_3 = m_1^2 - m_2^2 + m_3^2 = 2 m_1 E_3, \quad (13)$$

$$s = 2 p_2 \cdot p_3 = m_1^2 - m_2^2 - m_3^2, \quad (14)$$

$$s t + s u - t u = 4 m_1^2 p^2, \quad (15)$$

where the subscripts  $i = 1, 2$  and  $3$  of the variables (such as, four-dimensional momentum  $p_i$ , energy  $E_i$ , and mass  $m_i$ ) correspond to the  $\overline{B}_q^*$ ,  $D$  and  $M$  mesons, respectively.  $k_i$  is the momentum of the light antiquark carrying the longitudinal momentum fraction  $x_i$ .  $k_{iT}$  is the transverse momentum.  $t$ ,  $u$  and  $s$  are the Lorentz scalar variables.  $p$  is the common momentum of the final states. These momenta are shown in Fig.1(a), Fig.2(a) and Fig.3(a).

#### D. Wave functions

As aforementioned, wave functions are the essential input parameters in the master pQCD formula for the HME calculation. Following the notations in Refs. [36–43], the wave functions of the participating meson are defined as the meson-to-vacuum HME.

$$\langle 0 | \bar{q}_i(z) b_j(0) | \overline{B}_q^*(p, \epsilon^\parallel) \rangle = \frac{f_{B_q^*}}{4} \int d^4 k e^{-ik \cdot z} \left\{ \not{\epsilon}^\parallel \left[ m_{B_q^*} \Phi_{B_q^*}^v(k) - \not{p} \Phi_{B_q^*}^t(k) \right] \right\}_{ji}, \quad (16)$$

$$\langle 0 | \bar{q}_i(z) b_j(0) | \bar{B}_q^*(p, \epsilon^\perp) \rangle = \frac{f_{B_q^*}}{4} \int d^4 k e^{-ik \cdot z} \left\{ \not{\epsilon}^\perp \left[ m_{B_q^*} \Phi_{B_q^*}^V(k) - \not{k} \Phi_{B_q^*}^T(k) \right] \right\}_{ji}, \quad (17)$$

$$\langle D_q(p) | \bar{c}_i(0) q_j(z) | 0 \rangle = \frac{i f_{D_q}}{4} \int d^4 k e^{+ik \cdot z} \left\{ \gamma_5 \left[ \not{k} \Phi_{D_q}^a(k) + m_{D_q} \Phi_{D_q}^p(k) \right] \right\}_{ji}, \quad (18)$$

$$\begin{aligned} \langle P(p) | \bar{q}_i(0) q'_j(z) | 0 \rangle &= \frac{1}{4} \int d^4 k e^{+ik \cdot z} \left\{ \gamma_5 \left[ \not{k} \Phi_P^a(k) + \mu_P \Phi_P^p(k) \right. \right. \\ &\quad \left. \left. + \mu_P (\not{n}_+ \not{n}_- - 1) \Phi_P^t(k) \right] \right\}_{ji}, \end{aligned} \quad (19)$$

$$\langle V(p, \epsilon^\parallel) | \bar{q}_i(0) q'_j(z) | 0 \rangle = \frac{1}{4} \int d^4 k e^{+ik \cdot z} \left\{ \not{\epsilon}^\parallel m_V \Phi_V^v(k) + \not{\epsilon}^\parallel \not{k} \Phi_V^t(k) - m_V \Phi_V^s(k) \right\}_{ji}, \quad (20)$$

$$\begin{aligned} \langle V(p, \epsilon^\perp) | \bar{q}_i(0) q'_j(z) | 0 \rangle &= \frac{1}{4} \int d^4 k e^{+ik \cdot z} \left\{ \not{\epsilon}^\perp m_V \Phi_V^V(k) + \not{\epsilon}^\perp \not{k} \Phi_V^T(k) \right. \\ &\quad \left. + \frac{i m_V}{p \cdot n_+} \gamma_5 \varepsilon_{\mu\nu\alpha\beta} \gamma^\mu \epsilon^{\perp\nu} p^\alpha n_+^\beta \Phi_V^A(k) \right\}_{ji}, \end{aligned} \quad (21)$$

where  $f_{B_q^*}$  and  $f_{D_q}$  are the decay constants of the  $\bar{B}_q^*$  meson and the  $D_q$  meson, respectively.  $\epsilon^\parallel$  and  $\epsilon^\perp$  are the longitudinal and transverse polarization vectors.  $n_+ = (1, 0, 0)$  and  $n_- = (0, 1, 0)$  are the positive and negative null vectors, i.e.,  $n_\pm^2 = 0$ . The chiral factor  $\mu_P$  relates the pseudoscalar meson mass to the quark mass through the following way [41],

$$\mu_P = \frac{m_\pi^2}{m_u + m_d} = \frac{m_K^2}{m_{u,d} + m_s} \approx (1.6 \pm 0.2) \text{ GeV}. \quad (22)$$

With the twist classification based on the power counting rule in the infinite momentum frame [36, 37], the wave functions  $\Phi_{B_q^*, V}^{v, T}$  and  $\Phi_{D_q, P}^a$  are twist-2 (the leading twist), while the wave functions  $\Phi_{B_q^*, V}^{t, V, s, A}$  and  $\Phi_{D_q, P}^{p, t}$  are twist-3. By integrating out the transverse momentum from the wave functions, one can obtain the corresponding distribution amplitudes. In our calculation, the expressions of the DAs for the heavy-flavored mesons are [38–40]

$$\phi_{B_q^*}^{v, T}(x) = A x \bar{x} \exp \left\{ - \frac{1}{8 \omega_{B_q^*}^2} \left( \frac{m_q^2}{x} + \frac{m_b^2}{\bar{x}} \right) \right\}, \quad (23)$$

$$\phi_{B_q^*}^t(x) = B (\bar{x} - x)^2 \exp \left\{ - \frac{1}{8 \omega_{B_q^*}^2} \left( \frac{m_q^2}{x} + \frac{m_b^2}{\bar{x}} \right) \right\}, \quad (24)$$

$$\phi_{B_q^*}^V(x) = C \{1 + (\bar{x} - x)^2\} \exp \left\{ - \frac{1}{8 \omega_{B_q^*}^2} \left( \frac{m_q^2}{x} + \frac{m_b^2}{\bar{x}} \right) \right\}, \quad (25)$$

$$\phi_{D_q}^a(x) = D x \bar{x} \exp \left\{ - \frac{1}{8 \omega_{D_q}^2} \left( \frac{m_q^2}{x} + \frac{m_c^2}{\bar{x}} \right) \right\}, \quad (26)$$



$$\phi_{D_q}^p(x) = E \exp \left\{ - \frac{1}{8 \omega_{D_q}^2} \left( \frac{m_q^2}{x} + \frac{m_c^2}{\bar{x}} \right) \right\}, \quad (27)$$

where  $x$  and  $\bar{x} (\equiv 1 - x)$  are the longitudinal momentum fractions of the light and heavy partons;  $m_b$ ,  $m_c$  and  $m_q$  are the mass of the valence  $b$ ,  $c$  and  $q$  quarks. The parameter  $\omega_i$  determines the average transverse momentum of the partons, and  $\omega_i \approx m_i \alpha_s(m_i)$ . The parameters  $A$ ,  $B$ ,  $C$ ,  $D$  and  $E$  are the normalization coefficients to satisfy the conditions,

$$\int_0^1 dx \phi_{B_q^*}^{v,t,V,T}(x) = 1, \quad (28)$$

$$\int_0^1 dx \phi_{D_q}^{a,p}(x) = 1. \quad (29)$$

The main distinguishing feature of the above DAs in Eqs.(23-27) is the exponential functions, where the exponential factors are proportional to the ratio of the parton mass squared  $m_i^2$  to the momentum fraction  $x_i$ , i.e.,  $m_i^2/x_i$ . Hence, the DAs of Eqs.(23-27) are generally consistent with the ansatz that the momentum fractions are shared among the valence quarks according to the quark mass, i.e., a light quark will carry a smaller fraction of the parton momentum than a heavy quark in a heavy-light system. In addition, the exponential functions strongly suppress the contributions from the endpoint of  $x, \bar{x} \rightarrow 0$ , and naturally provide the effective truncation for the endpoint and soft contributions.

As is well known, there are many phenomenological DA models for the charmed mesons. Some have been recited by Eq.(30) in Ref.[30]. One of the favorable DA models from the experimental data, without the distinction between the twist-2 and twist-3, has the common expression as below,

$$\phi_{D_q}(x) = 6 x \bar{x} \{ 1 + C_{D_q} (\bar{x} - x) \}, \quad (30)$$

where the parameter  $C_{D_{u,d}} = 0.5$  for the  $D_{u,d}$  meson, and  $C_{D_s} = 0.4$  for the  $D_s$  meson.

The expressions of the twist-2 quark-antiquark DAs for the light pseudoscalar and vector mesons have the expansion [41–43],

$$\phi_P^a(x) = i f_P 6 x \bar{x} \sum_{i=0} a_i^P C_i^{3/2}(\xi), \quad (31)$$

$$\phi_V^v(x) = f_V 6 x \bar{x} \sum_{i=0} a_i^\parallel C_i^{3/2}(\xi), \quad (32)$$

$$\phi_V^T(x) = f_V^T 6 x \bar{x} \sum_{i=0} a_i^\perp C_i^{3/2}(\xi), \quad (33)$$

where  $f_P$  is the decay constant for the pseudoscalar meson  $P$ ;  $f_V$  and  $f_V^T$  are the vector and tensor (also called the longitudinal and transverse) decay constants for the vector meson  $V$ . The nonperturbative parameters of  $a_i^{P,\parallel,\perp}$  are called the Gegenbauer moments, and  $a_0^{P,\parallel,\perp} = 1$  for the asymptotic forms,  $a_{\text{odd } i}^{P,\parallel,\perp} = 0$  for the DAs of the  $G$ -parity eigenstates, such as the unflavored  $\pi$ ,  $\eta$ ,  $\eta'$ ,  $\rho$ ,  $\omega$ ,  $\phi$  mesons. The short-hand notation  $\xi = x - \bar{x} = 2x - 1$ . The analytical expressions of the Gegenbauer polynomials  $C_i^j(\xi)$  are as below,

$$C_0^j(\xi) = 1, \quad (34)$$

$$C_1^j(\xi) = 2j\xi, \quad (35)$$

$$C_2^j(\xi) = 2j(j+1)\xi^2 - j, \quad (36)$$

.....

As for the twist-3 DAs for the light pseudoscalar and vector mesons, their asymptotic forms will be employed in this paper for the simplification [30, 41–43], i.e.,

$$\phi_P^p(x) = +i f_P C_0^{1/2}(\xi), \quad (37)$$

$$\phi_P^t(x) = -i f_P C_1^{1/2}(\xi), \quad (38)$$

$$\phi_V^t(x) = +3 f_V^T \xi^2, \quad (39)$$

$$\phi_V^s(x) = -3 f_V^T \xi, \quad (40)$$

$$\phi_V^V(x) = +\frac{3}{4} f_V (1 + \xi^2), \quad (41)$$

$$\phi_V^A(x) = -\frac{3}{2} f_V \xi. \quad (42)$$

## E. Decay amplitudes

As aforementioned, the  $\overline{B}_q^* \rightarrow DM$  weak decays are induced practically by the  $b$  quark decay at the quark level. There are three possible types of Feynman diagrams for the  $\overline{B}_q^* \rightarrow DM$  decays with the pQCD approach, i.e., the color-allowed topologies of Fig.1 induced by the external  $W$ -emission interactions, the color-suppressed topologies of Fig.2 induced by the internal  $W$ -emission interactions, and the annihilation topologies of Fig.3 induced by the  $W$ -exchange interactions. In the emission topologies of Fig.1 (Fig.2), the light spectator quark in the  $\overline{B}_q^*$  meson is absorbed by the recoiled  $D_q$  ( $M_q$ ) meson, and the exchanged gluons are space-like. In the annihilation topologies of Fig.3, the exchanged gluons are time-like, which then split into the light quark-antiquark pair.

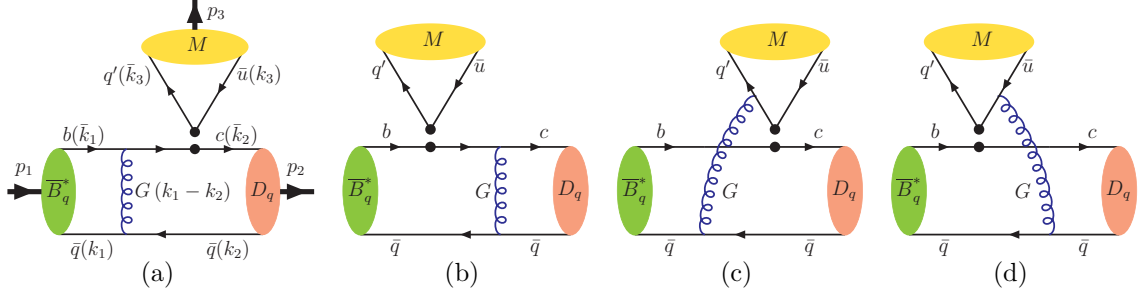


FIG. 1: The color-allowed diagrams for the  $\bar{B}_q^* \rightarrow D_q M$  decays with the pQCD approach, where (a,b) and (c,d) are factorizable and nonfactorizable emission topologies, respectively.

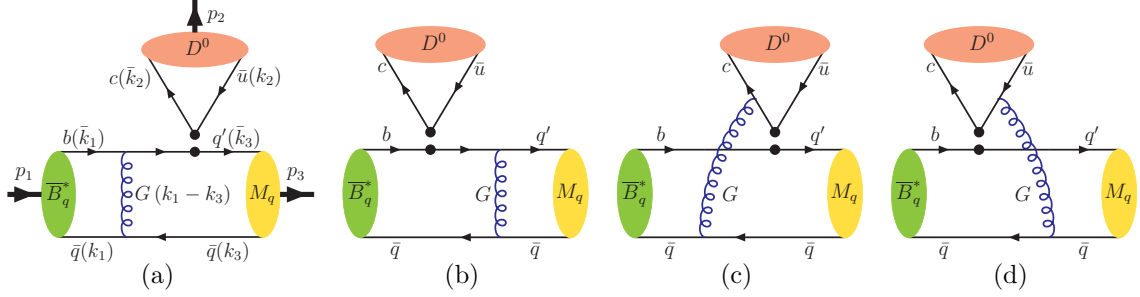


FIG. 2: The color-suppressed diagrams for the  $\bar{B}_q^* \rightarrow D^0 M_q$  decays with the pQCD approach.

The first two diagrams of Fig.1, Fig.2, and Fig.3 are usually called the factorizable topologies. In the color-allowed (color-suppressed) factorizable emission topologies, the gluons are exchanged only between the initial  $\bar{B}_q^*$  and the recoil  $D_q$  ( $M_q$ ) meson pair, and the emission  $M$  ( $D^0$ ) meson could be completely parted from the  $\bar{B}_q^* D_q$  ( $\bar{B}_q^* M_q$ ) system. In the factorizable annihilation topologies, the gluons are exchanged only between the final  $DM$  meson pair, and the initial  $\bar{B}_q^*$  meson could be directly separated from the  $DM$  meson pair. Hence, in the factorizable emission (annihilation) topologies, the integral of the wave functions for the emission (initial) mesons reduces to the corresponding decay constant. For the factorizable topologies, the decay amplitudes will have the relatively simple structures, and can be written as the product of the decay constants and the hadron transition form factors. With the pQCD approach, the form factors can be written as the convolution integral of the hard scattering amplitudes and the hadron DAs.

The last two diagrams of Fig.1, Fig.2, and Fig.3 are usually called the nonfactorizable topologies. In the nonfactorizable topologies, the emission meson is entangled with the gluons that radiated from the spectator quark, and hence on meson can be separated clearly from the other mesons. Hence, the decay amplitudes for the nonfactorizable topologies have quite complicated structures, and the amplitude convolution integral involve the wave

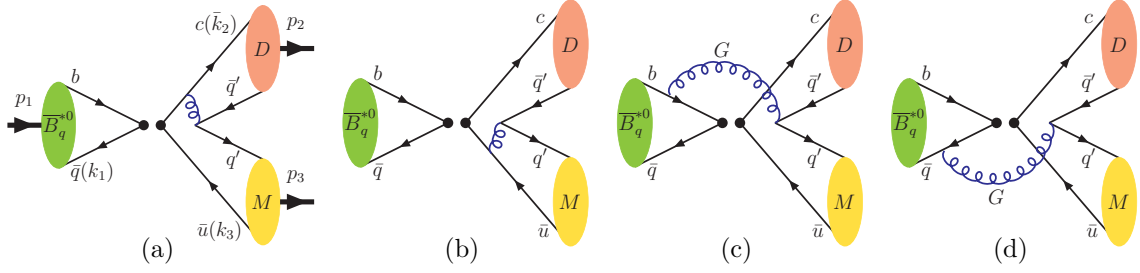


FIG. 3: The annihilation diagrams for the  $\bar{B}_q^{*0} \rightarrow DM$  decays with the pQCD approach.

functions of all the participating mesons. The nonfactorizable emission topologies within the pQCD framework are also called the spectator scattering topologies with the QCDF approach. Especially for the color-suppressed emission topologies, the factorizable contributions are proportional to the small parameter  $a_2$ , hence, the nonfactorizable contributions, being proportional to the large Wilson coefficient  $C_1$ , should be significant. As widely recognized, the nonfactorizable contributions play an important role in clarifying or reducing some discrepancies between the theoretical results and the experimental data on the nonleptonic  $B$  meson weak decays.

Among the three possible types of Feynman diagrams (Fig.1, Fig.2, and Fig.3), only one or two of them will contribute to the specific  $\bar{B}_q^* \rightarrow DM$  decays. The explicit amplitudes for the concrete  $\bar{B}_q^* \rightarrow DP$ ,  $DV$  decays have been collected in the Appendixes A and B, and the building blocks in the Appendixes C, D and E. According to the polarization relations between the initial and final vector mesons, the amplitudes for the  $\bar{B}_q^* \rightarrow DV$  decays can generally be decomposed into the following structures [44–47],

$$\mathcal{A}(\bar{B}_q^* \rightarrow DV) = \mathcal{A}_L(\epsilon_{B_q^*}^\parallel, \epsilon_V^\parallel) + \mathcal{A}_N(\epsilon_{B_q^*}^\perp \cdot \epsilon_V^\perp) + i \mathcal{A}_T \varepsilon_{\mu\nu\alpha\beta} \epsilon_{B_q^*}^\mu \epsilon_V^\nu p_{B_q^*}^\alpha p_V^\beta. \quad (43)$$

which is conventionally written as the helicity amplitudes,

$$H_0 = \mathcal{A}_L(\epsilon_{B_q^*}^\parallel, \epsilon_V^\parallel), \quad (44)$$

$$H_\parallel = \sqrt{2} \mathcal{A}_N, \quad (45)$$

$$H_\perp = \sqrt{2} m_{B_q^*} p \mathcal{A}_T. \quad (46)$$

As is well known, it is commonly assumed that the  $SU(3)$  symmetry breaking interactions mixes the isospin-singlet neutral members of the octet with the singlet states. The ideal mixing angle  $\theta_V$  (with  $\sin\theta_V = 1/\sqrt{3}$ ) between the octet and the singlet states is almost true in practice for the physical  $\omega$  and  $\phi$  mesons, i.e., the valence quark components are  $\omega$

$= (u\bar{u} + d\bar{d})/\sqrt{2}$  and  $\phi = s\bar{s}$ . As for the mixing among the light pseudoscalar mesons, the notations known as the quark-flavor basis description [48] is adopted here, and for simplicity, the possible gluonium and charmonium compositions are neglected for the time being, i.e.,

$$\begin{pmatrix} \eta \\ \eta' \end{pmatrix} = \begin{pmatrix} \cos\theta_P & -\sin\theta_P \\ \sin\theta_P & \cos\theta_P \end{pmatrix} \begin{pmatrix} \eta_q \\ \eta_s \end{pmatrix}, \quad (47)$$

where the flavor states  $\eta_q = (u\bar{u} + d\bar{d})/\sqrt{2}$  and  $\eta_s = s\bar{s}$ . The mixing angle determined from experimental data is  $\theta_P = (39.3 \pm 1.0)^\circ$  [48]. The mass relations between the physical states ( $\eta$  and  $\eta'$ ) and the flavor states ( $\eta_q$  and  $\eta_s$ ) are

$$m_{\eta_q}^2 = m_\eta^2 \cos^2\theta_P + m_{\eta'}^2 \sin^2\theta_P - \frac{\sqrt{2} f_{\eta_s}}{f_{\eta_q}} (m_{\eta'}^2 - m_\eta^2) \cos\theta_P \sin\theta_P, \quad (48)$$

$$m_{\eta_s}^2 = m_\eta^2 \sin^2\theta_P + m_{\eta'}^2 \cos^2\theta_P - \frac{f_{\eta_q}}{\sqrt{2} f_{\eta_s}} (m_{\eta'}^2 - m_\eta^2) \cos\theta_P \sin\theta_P, \quad (49)$$

where  $f_{\eta_q}$  and  $f_{\eta_s}$  are the decay constants.

The amplitudes for the  $\bar{B}_q^* \rightarrow D\eta$ ,  $D\eta'$  decays can be written as

$$\mathcal{A}(\bar{B}_q^* \rightarrow D\eta) = \cos\theta_P \mathcal{A}(\bar{B}_q^* \rightarrow D\eta_q) - \sin\theta_P \mathcal{A}(\bar{B}_q^* \rightarrow D\eta_s), \quad (50)$$

$$\mathcal{A}(\bar{B}_q^* \rightarrow D\eta') = \sin\theta_P \mathcal{A}(\bar{B}_q^* \rightarrow D\eta_q) + \cos\theta_P \mathcal{A}(\bar{B}_q^* \rightarrow D\eta_s). \quad (51)$$

### III. NUMERICAL RESULTS AND DISCUSSION

In the rest frame of the  $\bar{B}_q^*$  meson, the branching ratio is defined as

$$\mathcal{B}r(\bar{B}_q^* \rightarrow DV) = \frac{1}{24\pi} \frac{p}{m_{B_q^*}^2 \Gamma_{B_q^*}} \left\{ |H_0|^2 + |H_{\parallel}|^2 + |H_{\perp}|^2 \right\}, \quad (52)$$

$$\mathcal{B}r(\bar{B}_q^* \rightarrow DP) = \frac{1}{24\pi} \frac{p}{m_{B_q^*}^2 \Gamma_{B_q^*}} |\mathcal{A}(\bar{B}_q^* \rightarrow DP)|^2, \quad (53)$$

where  $\Gamma_{B_q^*}$  is the full decay width of the  $\bar{B}_q^*$  meson.

Unfortunately, the experimental data on  $\Gamma_{B_q^*}$  are still unavailable until now. As is generally known, the electromagnetic radiation processes  $\bar{B}_q^* \rightarrow \bar{B}_q \gamma$  dominate the  $\bar{B}_q^*$  meson decays, and the mass differences between the  $\bar{B}_q^*$  and  $\bar{B}_q$  mesons are very small,  $m_{B_q^*} - m_{B_q} \lesssim 50$  MeV [1], which results in the fact that the photons from the  $\bar{B}_q^* \rightarrow \bar{B}_q \gamma$  process are too soft to be easily identified by the detectors at the existing experiments. A good approximation for the decay width is  $\Gamma_{B_q^*} \approx \Gamma(\bar{B}_q^* \rightarrow \bar{B}_q \gamma)$ . Theoretically, there is the close

relation between the partial decay width for the  $\overline{B}_q^* \rightarrow \overline{B}_q \gamma$  decay and the magnetic dipole (M1) moment of the  $\overline{B}_q^*$  meson [32], i.e.,

$$\Gamma(\overline{B}_q^* \rightarrow \overline{B}_q \gamma) = \frac{4}{3} \alpha_{\text{em}} k_\gamma^3 \mu_h^2, \quad (54)$$

where  $\alpha_{\text{em}}$  is the fine structure constant;  $k_\gamma = (m_{B_q^*}^2 - m_{B_q}^2)/2m_{B_q^*}$  is the photon momentum in the rest frame of the  $\overline{B}_q^*$  meson;  $\mu_h$  is the M1 moment of the  $\overline{B}_q^*$  meson. There are a large number of theoretical predictions on the partial decay width  $\Gamma(\overline{B}_q^* \rightarrow \overline{B}_q \gamma)$ . Many of these have been collected into Table 7 of Ref.[49] and Tables 3 and 4 of Ref.[32]. However, there are big differences among these estimations with various models, due to our inaccurate information about the M1 moments of mesons. In principle, the M1 moment of a hadron should be the sum of the M1 moments of its constituent quarks. As is well known, for an elementary particle, the M1 moment is proportional to the charge and inversely proportional to the mass. Hence, the M1 moment of the heavy-light  $\overline{B}_q^*$  meson should be mainly affected by the M1 moment of the light quark rather than the bottom quark. With the M1 moments of the light  $u$ ,  $d$  and  $s$  quarks in the terms of the nuclear magnetons  $\mu_N$ , i.e.,  $\mu_u \simeq 1.85 \mu_N$ ,  $\mu_d \simeq -0.97 \mu_N$ , and  $\mu_s \simeq -0.61 \mu_N$  [50], it is expected to have the relations  $\Gamma(\overline{B}_u^* \rightarrow \overline{B}_u \gamma) > \Gamma(\overline{B}_d^* \rightarrow \overline{B}_d \gamma) > \Gamma(\overline{B}_s^* \rightarrow \overline{B}_s \gamma)$ , and therefore the relations  $\Gamma_{B_u^*} > \Gamma_{B_d^*} > \Gamma_{B_s^*}$ . It is far beyond the scope of this paper to elaborate more on the details of the decay width  $\Gamma_{B_q^*}$ . In our calculation, in order to give a quantitative estimation of the branching ratios for the  $\overline{B}_q^* \rightarrow DM$  decays, we will use the following values of the decay widths,

$$\Gamma_{B_u^*} \sim \Gamma(\overline{B}_u^* \rightarrow \overline{B}_u \gamma) \sim 450 \text{ eV}, \quad (55)$$

$$\Gamma_{B_d^*} \sim \Gamma(\overline{B}_d^* \rightarrow \overline{B}_d \gamma) \sim 150 \text{ eV}, \quad (56)$$

$$\Gamma_{B_s^*} \sim \Gamma(\overline{B}_s^* \rightarrow \overline{B}_s \gamma) \sim 100 \text{ eV}, \quad (57)$$

which is basically consistent with the recent results of Ref.[32].

The numerical values of other input parameters are collected in Table I, where their central values will be fixed as the default inputs unless otherwise specified. In addition, in order to investigate the effects from different DA models, we explore three scenarios,

- Scenario I: Eqs.(23-27) for the DAs of  $\phi_{B^*}^{v,t,V,T}$  and  $\phi_{D_q}^{a,p}$ ;
- Scenario II:  $\phi_{B^*}^{v,t,V,T} = \text{Eq.}(23)$ , and  $\phi_{D_q}^{a,p} = \text{Eq.}(26)$ ;

TABLE I: The numerical values of input parameters.

CKM parameter	$A = 0.811 \pm 0.026$ [1],	$\lambda = 0.22506 \pm 0.00050$ [1],
mass of the particles	$m_{\pi^\pm} = 139.57$ MeV [1],	$m_{K^\pm} = 493.677 \pm 0.016$ MeV [1],
$m_b = 4.78 \pm 0.06$ GeV [1],	$m_{\pi^0} = 134.98$ MeV [1],	$m_{K^0} = 497.611 \pm 0.013$ MeV [1],
$m_c = 1.67 \pm 0.07$ GeV [1],	$m_{\eta'} = 957.78 \pm 0.06$ MeV [1],	$m_\eta = 547.862 \pm 0.017$ MeV [1],
$m_s \simeq 0.51$ GeV [50],	$m_\rho = 775.26 \pm 0.25$ MeV [1],	$m_{K^{*0}} = 895.81 \pm 0.19$ MeV [1],
$m_{u,d} \simeq 0.31$ GeV [50],	$m_\omega = 782.62 \pm 0.12$ MeV [1],	$m_{K^{*\pm}} = 891.66 \pm 0.26$ MeV [1],
$m_{B_s^*} = 5415.4_{-1.5}^{+1.8}$ MeV [1],	$m_{B_{u,d}^*} = 5324.65 \pm 0.25$ MeV [1],	$m_\phi = 1019.461 \pm 0.019$ MeV [1],
$m_{D_s} = 1968.27 \pm 0.10$ MeV [1],	$m_{D_d} = 1869.58 \pm 0.09$ MeV [1],	$m_{D_u} = 1864.83 \pm 0.05$ MeV [1],
decay constant	$f_\pi = 130.2 \pm 1.7$ MeV [1],	$f_K = 155.6 \pm 0.4$ MeV [1],
$f_{\eta_q} = (1.07 \pm 0.02) f_\pi$ [48],	$f_{K^*} = 220 \pm 5$ MeV [42],	$f_{K^*}^T = 185 \pm 10$ MeV [42],
$f_{\eta_s} = (1.34 \pm 0.06) f_\pi$ [48],	$f_\rho = 216 \pm 3$ MeV [42],	$f_\rho^T = 165 \pm 9$ MeV [42],
$f_{D_s} = 249.0 \pm 1.2$ MeV [1],	$f_\omega = 187 \pm 5$ MeV [42],	$f_\omega^T = 151 \pm 9$ MeV [42],
$f_{D_{u,d}} = 211.9 \pm 1.1$ MeV [1],	$f_\phi = 215 \pm 5$ MeV [42],	$f_\phi^T = 186 \pm 9$ MeV [42],
$f_{B_s^*} = 213 \pm 7$ MeV [51],	$f_{B_{u,d}^*} = 175 \pm 6$ MeV [51],	
Gegenbauer moment	$a_2^{\pi, \eta_q, s} = 0.25 \pm 0.15$ [43],	$a_2^{\parallel, \rho, \omega} = 0.15 \pm 0.07$ [42],
$a_1^K = -0.06 \pm 0.03$ [43],	$a_2^K = 0.25 \pm 0.15$ [43],	$a_2^{\perp, \rho, \omega} = 0.14 \pm 0.06$ [42],
$a_1^{\parallel, K^*} = -0.03 \pm 0.02$ [42],	$a_2^{\parallel, K^*} = 0.11 \pm 0.09$ [42],	$a_2^{\parallel, \phi} = 0.18 \pm 0.08$ [42],
$a_1^{\perp, K^*} = -0.04 \pm 0.03$ [42],	$a_2^{\perp, K^*} = 0.10 \pm 0.08$ [42],	$a_2^{\perp, \phi} = 0.14 \pm 0.07$ [42].

- Scenario III:  $\phi_{B^*}^{v,t,V,T} = \text{Eq.}(23)$ , and  $\phi_{D_q}^{a,p} = \text{Eq.}(30)$ .

Our numerical results on the branching ratios are presented in Tables II and III, where the uncertainties come from the typical scale  $(1 \pm 0.1)t_i$ , the mass  $m_c$  and  $m_b$ , and the hadronic parameters (including the decay constants, Gegenbauer moments, and so on), respectively. The following are some comments.

(1) Generally, the  $\overline{B}_q^* \rightarrow DP$  decay modes could be divided into three categories, i.e. the “T”, “C”, and “A” types are dominated by contributions from the color-allowed emission topologies of Fig.1, the color-suppressed emission topologies of Fig.2, and the pure annihilation topologies of Fig.3, respectively. And each category could be further divided into two classes, i.e., the decay amplitudes of the classes “I” and “II” are proportional to the

TABLE II: The branching ratios for the  $\overline{B}_q^* \rightarrow DP$  decays with the different DA scenarios, where the theoretical uncertainties come from the scale  $(1 \pm 0.1)t_i$ , the mass  $m_c$  and  $m_b$ , and the hadronic parameters (including the decay constants, Gegenbauer moments, and so on).

decay mode	class	unit	I	II	III
$B_u^{*-} \rightarrow D_u^0 \pi^-$	T-I	$10^{-10}$	$6.61^{+2.12+0.07+0.75}_{-0.92-0.79-0.69}$	$1.25^{+0.25+0.11+0.16}_{-0.13-0.13-0.15}$	$0.56^{+0.13+0.09+0.08}_{-0.07-0.09-0.07}$
$B_u^{*-} \rightarrow D_u^0 K^-$	T-II	$10^{-11}$	$5.38^{+1.97+0.05+0.55}_{-0.85-0.63-0.51}$	$0.95^{+0.20+0.09+0.11}_{-0.10-0.10-0.10}$	$0.42^{+0.10+0.07+0.05}_{-0.05-0.07-0.05}$
$\overline{B}_d^{*0} \rightarrow D_d^+ \pi^-$	T-I	$10^{-9}$	$2.22^{+0.52+0.02+0.27}_{-0.20-0.23-0.24}$	$0.51^{+0.08+0.04+0.07}_{-0.03-0.05-0.06}$	$0.28^{+0.04+0.03+0.04}_{-0.02-0.04-0.03}$
$\overline{B}_d^{*0} \rightarrow D_d^+ K^-$	T-II	$10^{-10}$	$1.69^{+0.38+0.01+0.15}_{-0.15-0.18-0.14}$	$0.38^{+0.06+0.03+0.03}_{-0.02-0.03-0.03}$	$0.20^{+0.03+0.03+0.02}_{-0.01-0.03-0.02}$
$\overline{B}_d^{*0} \rightarrow D_u^0 \pi^0$	C-I	$10^{-12}$	$4.04^{+3.19+0.38+1.32}_{-2.47-0.39-1.05}$	$6.11^{+0.81+0.32+1.72}_{-0.44-0.29-1.28}$	$7.21^{+1.02+0.13+1.66}_{-0.88-0.09-1.35}$
$\overline{B}_d^{*0} \rightarrow D_u^0 \eta$	C-I	$10^{-12}$	$3.48^{+2.78+0.21+0.80}_{-2.29-0.11-1.28}$	$4.49^{+0.63+0.36+0.98}_{-0.43-0.25-0.84}$	$3.60^{+0.73+0.22+0.68}_{-0.71-0.16-0.60}$
$\overline{B}_d^{*0} \rightarrow D_u^0 \eta'$	C-I	$10^{-12}$	$2.26^{+1.80+0.13+0.67}_{-1.49-0.07-0.72}$	$2.91^{+0.41+0.23+0.68}_{-0.28-0.16-0.56}$	$2.33^{+0.47+0.14+0.49}_{-0.46-0.10-0.41}$
$\overline{B}_d^{*0} \rightarrow D_u^0 \overline{K}^0$	C-II	$10^{-13}$	$2.19^{+4.55+0.72+2.30}_{-0.44-0.51-1.40}$	$9.66^{+1.59+0.72+2.86}_{-1.16-0.50-2.14}$	$9.54^{+1.94+0.39+1.96}_{-1.92-0.27-1.72}$
$\overline{B}_d^{*0} \rightarrow D_s^+ K^-$	A-I	$10^{-12}$	$0.64^{+0.05+0.17+1.09}_{-0.04-0.16-0.42}$	$1.30^{+0.06+0.10+0.89}_{-0.01-0.09-0.40}$	$0.40^{+0.05+0.03+0.20}_{-0.01-0.03-0.08}$
$\overline{B}_s^{*0} \rightarrow D_s^+ \pi^-$	T-I	$10^{-9}$	$5.68^{+1.17+0.09+0.60}_{-0.46-0.50-0.56}$	$1.48^{+0.21+0.07+0.16}_{-0.09-0.12-0.15}$	$0.81^{+0.11+0.07+0.09}_{-0.05-0.09-0.08}$
$\overline{B}_s^{*0} \rightarrow D_s^+ K^-$	T-II	$10^{-10}$	$4.30^{+0.89+0.09+0.40}_{-0.35-0.37-0.38}$	$1.17^{+0.17+0.06+0.12}_{-0.07-0.09-0.11}$	$0.64^{+0.09+0.06+0.06}_{-0.04-0.07-0.06}$
$\overline{B}_s^{*0} \rightarrow D_d^+ \pi^-$	A-II	$10^{-14}$	$0.16^{+0.17+0.75+2.36}_{-0.02-0.15-0.08}$	$1.71^{+0.31+0.48+2.44}_{-0.05-0.46-0.40}$	$1.80^{+0.58+0.10+2.08}_{-0.24-0.10-0.58}$
$\overline{B}_s^{*0} \rightarrow D_u^0 \pi^0$	A-II	$10^{-14}$	$0.08^{+0.09+0.38+1.19}_{-0.01-0.08-0.04}$	$0.86^{+0.16+0.24+1.23}_{-0.03-0.23-0.20}$	$0.90^{+0.29+0.05+1.05}_{-0.12-0.05-0.29}$
$\overline{B}_s^{*0} \rightarrow D_u^0 \eta$	C-II	$10^{-12}$	$0.20^{+0.38+0.06+0.15}_{-0.02-0.06-0.09}$	$0.90^{+0.16+0.05+0.26}_{-0.12-0.07-0.20}$	$1.01^{+0.21+0.01+0.27}_{-0.21-0.03-0.22}$
$\overline{B}_s^{*0} \rightarrow D_u^0 \eta'$	C-II	$10^{-12}$	$0.36^{+0.72+0.10+0.21}_{-0.08-0.08-0.16}$	$1.38^{+0.24+0.08+0.31}_{-0.19-0.09-0.31}$	$1.22^{+0.30+0.02+0.23}_{-0.30-0.06-0.26}$
$\overline{B}_s^{*0} \rightarrow D_u^0 K^0$	C-I	$10^{-11}$	$3.31^{+2.07+0.12+1.09}_{-1.88-0.24-0.77}$	$4.31^{+0.51+0.16+1.22}_{-0.28-0.25-0.93}$	$4.21^{+0.61+0.02+0.94}_{-0.53-0.16-0.80}$

CKM factors of  $V_{cb} V_{ud}^* \sim \Lambda \lambda^2$  and  $V_{cb} V_{us}^* \sim \Lambda \lambda^3$ , respectively. There are many hierarchical relations among the branching ratios, such as,

$$\mathcal{Br}(\text{class T-I}) > \mathcal{Br}(\text{class C-I}) > \mathcal{Br}(\text{class A-I}), \quad (58)$$

$$\mathcal{Br}(\text{class T-II}) > \mathcal{Br}(\text{class C-II}) > \mathcal{Br}(\text{class A-II}), \quad (59)$$

$$\mathcal{Br}(\text{class X-I}) > \mathcal{Br}(\text{class X-II}), \quad \text{for } X = \text{T, C, A}. \quad (60)$$

These categories and relations also happen to hold true for the  $\overline{B}_q^* \rightarrow DV$  decays.

For the “T” and “C” types of the  $\overline{B}_q^* \rightarrow DM$  decays, the annihilation contributions have a negligible impact on the branching ratios, and they are strongly suppressed relative to the emission contributions, as is stated by the QCDF approach [13].



TABLE III: The branching ratios for the  $\overline{B}_q^* \rightarrow DV$  decays with the different DA scenarios, where the theoretical uncertainties arise from the scale  $(1 \pm 0.1)t_i$ , the mass  $m_c$  and  $m_b$ , and the hadronic parameters (including the decay constants, Gegenbauer moments, and so on).

decay mode	class	unit	Scenario I	Scenario II	Scenario III
$B_u^{*-} \rightarrow D_u^0 \rho^-$	T-I	$10^{-9}$	$2.02^{+0.55+0.02+0.23}_{-0.23-0.22-0.21}$	$0.43^{+0.08+0.04+0.05}_{-0.04-0.04-0.05}$	$0.19^{+0.04+0.03+0.02}_{-0.02-0.03-0.02}$
$B_u^{*-} \rightarrow D_u^0 K^{*-}$	T-II	$10^{-10}$	$1.14^{+0.32+0.01+0.16}_{-0.13-0.13-0.14}$	$0.25^{+0.05+0.02+0.04}_{-0.02-0.03-0.03}$	$0.11^{+0.02+0.02+0.02}_{-0.01-0.02-0.01}$
$\overline{B}_d^{*0} \rightarrow D_d^+ \rho^-$	T-I	$10^{-9}$	$6.80^{+1.55+0.03+0.79}_{-0.60-0.66-0.72}$	$1.72^{+0.26+0.11+0.21}_{-0.11-0.15-0.19}$	$0.95^{+0.13+0.11+0.11}_{-0.06-0.11-0.10}$
$\overline{B}_d^{*0} \rightarrow D_d^+ K^{*-}$	T-II	$10^{-10}$	$3.87^{+0.87+0.01+0.51}_{-0.33-0.36-0.46}$	$0.99^{+0.15+0.07+0.13}_{-0.06-0.09-0.12}$	$0.53^{+0.07+0.07+0.07}_{-0.03-0.07-0.07}$
$\overline{B}_d^{*0} \rightarrow D_u^0 \rho^0$	C-I	$10^{-11}$	$2.55^{+1.26+0.15+0.57}_{-1.06-0.09-0.47}$	$4.60^{+0.61+0.15+0.84}_{-0.44-0.09-0.72}$	$5.95^{+0.79+0.23+1.14}_{-0.76-0.19-0.98}$
$\overline{B}_d^{*0} \rightarrow D_u^0 \omega$	C-I	$10^{-11}$	$2.43^{+1.00+0.17+0.75}_{-0.79-0.11-0.60}$	$4.32^{+0.51+0.21+1.11}_{-0.35-0.15-0.91}$	$4.71^{+0.64+0.16+1.14}_{-0.62-0.14-0.94}$
$\overline{B}_d^{*0} \rightarrow D_u^0 \overline{K}^{*0}$	C-II	$10^{-12}$	$3.58^{+1.77+0.22+1.14}_{-1.52-0.16-0.89}$	$6.26^{+0.90+0.32+1.70}_{-0.70-0.25-1.40}$	$7.83^{+1.16+0.28+2.17}_{-1.16-0.29-1.76}$
$\overline{B}_d^{*0} \rightarrow D_s^+ K^{*-}$	A-I	$10^{-12}$	$5.55^{+0.94+0.50+2.57}_{-0.46-0.48-1.68}$	$6.82^{+0.58+0.54+2.09}_{-0.13-0.49-1.43}$	$3.98^{+0.54+0.10+1.19}_{-0.18-0.08-0.78}$
$\overline{B}_s^{*0} \rightarrow D_s^+ \rho^-$	T-I	$10^{-8}$	$1.72^{+0.35+0.03+0.19}_{-0.14-0.13-0.17}$	$0.50^{+0.07+0.03+0.05}_{-0.03-0.04-0.05}$	$0.27^{+0.04+0.02+0.03}_{-0.02-0.03-0.03}$
$\overline{B}_s^{*0} \rightarrow D_s^+ K^{*-}$	T-II	$10^{-9}$	$1.00^{+0.21+0.02+0.13}_{-0.08-0.09-0.12}$	$0.31^{+0.05+0.02+0.04}_{-0.02-0.03-0.04}$	$0.17^{+0.02+0.01+0.02}_{-0.01-0.02-0.02}$
$\overline{B}_s^{*0} \rightarrow D_d^+ \rho^-$	A-II	$10^{-13}$	$2.39^{+0.79+0.47+0.90}_{-0.31-0.20-0.53}$	$6.23^{+0.26+0.86+1.27}_{-0.00-0.72-0.91}$	$2.88^{+0.31+0.13+0.50}_{-0.04-0.11-0.36}$
$\overline{B}_s^{*0} \rightarrow D_u^0 \rho^0$	A-II	$10^{-13}$	$1.19^{+0.40+0.24+0.45}_{-0.15-0.10-0.27}$	$3.12^{+0.13+0.43+0.63}_{-0.00-0.36-0.45}$	$1.44^{+0.15+0.06+0.25}_{-0.02-0.05-0.18}$
$\overline{B}_s^{*0} \rightarrow D_u^0 \omega$	A-II	$10^{-13}$	$0.97^{+0.33+0.19+0.37}_{-0.13-0.08-0.22}$	$2.42^{+0.11+0.34+0.55}_{-0.00-0.28-0.40}$	$1.12^{+0.12+0.05+0.23}_{-0.02-0.04-0.17}$
$\overline{B}_s^{*0} \rightarrow D_u^0 \phi$	C-II	$10^{-11}$	$0.79^{+0.32+0.03+0.18}_{-0.30-0.04-0.15}$	$1.20^{+0.17+0.04+0.26}_{-0.13-0.04-0.22}$	$1.50^{+0.22+0.02+0.31}_{-0.21-0.04-0.27}$
$\overline{B}_s^{*0} \rightarrow D_u^0 K^{*0}$	C-I	$10^{-10}$	$1.69^{+0.67+0.07+0.51}_{-0.61-0.09-0.41}$	$2.58^{+0.32+0.07+0.70}_{-0.23-0.09-0.57}$	$3.19^{+0.42+0.05+0.87}_{-0.40-0.11-0.71}$

For the “T” types of the  $\overline{B}_q^* \rightarrow DM$  decays, the factorizable contributions from the emission topologies to the branching ratios are dominant over other contributions. However, for the “C” types of the  $\overline{B}_q^* \rightarrow DM$  decays, the nonfactorizable contributions to the branching ratios become very important, and sometimes even dominant.

(2) With the law of conservation of angular momentum, three partial wave amplitudes, including the  $s$ -,  $p$ -, and  $d$ -wave amplitudes, all will contribute to the  $\overline{B}_q^* \rightarrow DV$  decays, while only the  $p$ -wave amplitude will contribute to the  $\overline{B}_q^* \rightarrow DP$  decays. Besides, the branching ratios are proportional to the squares of the decay constants with the pQCD approach. With the magnitude relations between the decay constants  $f_V > f_P$ , one should

expect to have the general relation of the branching ratios,

$$\mathcal{Br}(\overline{B}_q^* \rightarrow DV) > \mathcal{Br}(\overline{B}_q^* \rightarrow DP), \quad (61)$$

for the final vector  $V$  and pseudoscalar  $P$  mesons carrying the same flavor, azimuthal and magnetic isospin quantum numbers. And due to the relations between the decay constants  $f_{B_s^*} > f_{B_{u,d}^*}$  and  $f_{D_s} > f_{D_{u,d}}$ , and the relations between the decay widths  $\Gamma_{B_s^*} < \Gamma_{B_{u,d}^*}$ , the color-allowed  $\overline{B}_s^{*0} \rightarrow D_s^+ \rho^-$  decay has a relatively large branching ratio.

Furthermore, our study results show that for the “T” types of the  $\overline{B}_q^* \rightarrow DV$  decays, the contributions of the longitudinal polarization part are dominant. Take the  $\overline{B}_s^{*0} \rightarrow D_s^+ \rho^-$  decay for example, the longitudinal polarization fraction  $f_0 \equiv \frac{|H_0|^2}{|H_0|^2 + |H_{||}|^2 + |H_{\perp}|^2} \approx 90\%$  (85%), the parallel polarization fraction  $f_{||} \equiv \frac{|H_{||}|^2}{|H_{||}|^2 + |H_{\perp}|^2} \approx 9\%$  (12%), and the perpendicular polarization fraction  $f_{\perp} \equiv \frac{|H_{\perp}|^2}{|H_{\perp}|^2 + |H_{||}|^2} \approx 1\%$  (3%) with the DA scenarios I (II and III), which generally agree with those obtained by the QCDF approach [31].

(3) As is well known, the theoretical results depend on the values of the input parameters. From the numbers in Tables II and III, it is clearly seen that the main uncertainty is due to the limited knowledge of the hadron DAs, for example, the large discrepancy among the different DA scenarios. Besides the theoretical uncertainties listed in Tables II and III, the CKM parameters will bring some 6% uncertainties. With a different value of the decay width  $\Gamma_{B_q^*}$ , the branching ratios in Tables II and III should be multiplied by the factors of  $450 \text{ eV}/\Gamma_{B_u^*}$ ,  $150 \text{ eV}/\Gamma_{B_d^*}$ ,  $100 \text{ eV}/\Gamma_{B_s^*}$  for the  $B_u^*$ ,  $B_d^*$ ,  $B_s^*$  weak decays, respectively. To reduce the theoretical uncertainties, one of the commonly used methods is to exploit the rate of the branching ratios, such as,

$$\frac{\mathcal{Br}(\overline{B}_u^{*-} \rightarrow D_u^0 \pi^-)}{\mathcal{Br}(\overline{B}_u^{*-} \rightarrow D_u^0 K^-)} \approx \frac{f_{\pi}^2}{\lambda^2 f_K^2}, \quad (62)$$

$$\frac{\mathcal{Br}(\overline{B}_u^{*-} \rightarrow D_u^0 \rho^-)}{\mathcal{Br}(\overline{B}_u^{*-} \rightarrow D_u^0 K^{*-})} \approx \frac{f_{\rho}^2}{\lambda^2 f_{K^*}^2}, \quad (63)$$

$$\frac{\mathcal{Br}(\overline{B}_s^{*0} \rightarrow D_u^0 \phi)}{\mathcal{Br}(\overline{B}_s^{*0} \rightarrow D_u^0 K^{*0})} \approx \frac{\lambda^2 f_{\phi}^2}{f_{K^*}^2}. \quad (64)$$

(4) The branching ratios for the  $\overline{B}_q^* \rightarrow DM$  decays are smaller by at least five orders of magnitude than the branching ratios for the  $\overline{B}_q \rightarrow DM$  decays [30]. This fact implies that the possible background from the  $\overline{B}_q^* \rightarrow DM$  decays could be safely neglected when the  $\overline{B}_q \rightarrow DM$  decays were analyzed, but not vice versa, i.e., one of main pollution backgrounds

for the  $\overline{B}_q^* \rightarrow DM$  decays would come from the  $\overline{B}_q \rightarrow DM$  decays, even if the invariant mass of the  $DM$  meson pair could be used to distinguish the  $\overline{B}_q^*$  meson from the  $\overline{B}_q$  meson experimentally.

TABLE IV: The channel fractions at the  $\Upsilon(5S)$  resonance [52].

channels	%/ $b\bar{b}$ event	%/ $B_s$ event
All $B_s$ events	$19.5^{+3.0}_{-2.3}$	
$B_s^{*0}\overline{B}_s^{*0}$		$90.1^{+3.8}_{-4.0}\pm 0.2$
$B_s^{*0}\overline{B}_s^0 + \text{c.c.}$		$7.3^{+3.3}_{-3.0}\pm 0.1$
$B^*\overline{B}^*$	$37.5^{+2.1}_{-1.9}\pm 3.0$	
$B^*\overline{B} + \text{c.c.}$	$13.7\pm 1.3\pm 1.1$	
$B^*\overline{B}\pi + \text{c.c.}$	$7.3^{+2.3}_{-2.1}\pm 0.8$	
$B^*\overline{B}^*\pi$	$1.0^{+1.4}_{-1.3}\pm 0.4$	

(5) The event numbers of the  $B_q^*$  meson in a data sample can be calculated by the following formula,

$$N(B_q^*) = \mathcal{L}_{\text{int}} \times \sigma_{b\bar{b}} \times f_{B_q} \times \frac{f_{B_q^*}}{f_{B_q}}. \quad (65)$$

$$f_{B_q^*} = 2 \times f_{B_q^*\overline{B}_q^*} + 2 \times f_{B_q^*\overline{B}_q^*\pi} + f_{B_q^*\overline{B}_q + \text{c.c.}} + f_{B_q^*\overline{B}_q\pi + \text{c.c.}} + \dots, \quad (66)$$

where  $\mathcal{L}_{\text{int}}$  is the integrated luminosity,  $\sigma_{b\bar{b}}$  denotes the  $b\bar{b}$  pair production cross section,  $f_{B_q}$ ,  $f_{B_q^*\overline{B}_q^*}$ ,  $\dots$  refer to the production fraction of all the  $B_q$  meson, the  $B_q^*\overline{B}_q^*$  meson pair,  $\dots$ . The production fractions of specific modes at the center-of-mass of the  $\Upsilon(5S)$  resonance [52] are listed in Table IV. With a large production cross section of the process  $e^+e^- \rightarrow b\bar{b}$  at the  $\Upsilon(5S)$  peak  $\sigma_{b\bar{b}} = (0.340 \pm 0.016)$  nb [52], it is expected that some  $3.3 \times 10^9$   $B_{u,d}^*$  and  $1.2 \times 10^9$   $B_s^*$  mesons could be available per  $10 \text{ ab}^{-1}$   $\Upsilon(5S)$  dataset. The branching ratios of the color-allowed “T-I” class  $\overline{B}_q^* \rightarrow DM$  decays can reach up to  $\mathcal{O}(10^{-9})$  or more, which are essentially coincident with those obtained by the QCDF approach [31]. Hence, a few events of the  $\overline{B}_q^* \rightarrow D_q\pi^-$  and  $\overline{B}_{u,d}^* \rightarrow D_{u,d}\rho^-$  decays, and dozens of the  $\overline{B}_s^{*0} \rightarrow D_s^+\rho^-$  decay, might be available at the forthcoming SuperKEKB. At high energy hadron colliders, for example, given with the cross section at the LHCb  $\sigma_{b\bar{b}} \approx 100 \mu\text{b}$  [1, 53, 54], with a similar ratio  $f_{B_u} = f_{B_d} = 0.344 \pm 0.021$  and  $f_{B_s} = 0.115 \pm 0.013$  at Tevatron [1, 55] and a similar ratio  $f_{B_q^*}/f_{B_q}$  at the  $\Upsilon(5S)$  meson [52], some  $9.8 \times 10^{13}$   $B_{u,d}^*$  events and  $2.2 \times 10^{13}$   $B_s^*$  events per  $\text{ab}^{-1}$  dataset

could be available at the LHCb, corresponding to more than  $10^5$  of the  $\overline{B}_s^{*0} \rightarrow D_s^+ \rho^-$  decay events and over  $10^4$  of the  $\overline{B}_q^* \rightarrow D_q \pi^-$  and  $\overline{B}_{u,d}^* \rightarrow D_{u,d} \rho^-$  decay events, which should be easily measured by the future LHCb experiments.

#### IV. SUMMARY

Besides the dominant electromagnetic decay mode, the ground vector  $B_q^*$  meson ( $q = u, d$  and  $s$ ) can also decay via the weak interactions within the standard model. A large amount of the  $B_q^*$  mesons are expected to be accumulated with the running LHC and the forthcoming SuperKEKB, which makes it seemingly possible to explore the  $B_q^*$  meson weak decays experimentally. The theoretical study is necessary to offer a ready reference. In this paper, we investigated the  $\overline{B}_q^* \rightarrow DP, DV$  decays with the phenomenological pQCD approach. It is found that the color-allowed  $\overline{B}_q^* \rightarrow D_q \rho^-$  decays have branching ratios  $\gtrsim 10^{-9}$ , and should be promisingly accessible at the high luminosity experiments in the future.

#### Acknowledgments

The work is supported by the National Natural Science Foundation of China (Grant Nos. U1632109, 11547014 and 11475055).

#### Appendix A: The amplitude for the $\overline{B}_q^* \rightarrow DP$ decays

$$\mathcal{A}(B_u^{*-} \rightarrow D_u^0 \pi^-) = \mathcal{F} V_{cb} V_{ud}^* \left\{ \sum_i \mathcal{M}_{i,P}^T + \sum_j \mathcal{M}_{j,P}^C \right\}, \quad (\text{A1})$$

$$\mathcal{A}(B_u^{*-} \rightarrow D_u^0 K^-) = \mathcal{F} V_{cb} V_{us}^* \left\{ \sum_i \mathcal{M}_{i,P}^T + \sum_j \mathcal{M}_{j,P}^C \right\}, \quad (\text{A2})$$

$$\mathcal{A}(\overline{B}_d^{*0} \rightarrow D_d^+ \pi^-) = \mathcal{F} V_{cb} V_{ud}^* \left\{ \sum_i \mathcal{M}_{i,P}^T + \sum_j \mathcal{M}_{j,P}^A \right\}, \quad (\text{A3})$$

$$\mathcal{A}(\overline{B}_d^{*0} \rightarrow D_d^+ K^-) = \mathcal{F} V_{cb} V_{us}^* \sum_i \mathcal{M}_{i,P}^T, \quad (\text{A4})$$

$$\sqrt{2} \mathcal{A}(\overline{B}_d^{*0} \rightarrow D_u^0 \pi^0) = \mathcal{F} V_{cb} V_{ud}^* \left\{ - \sum_i \mathcal{M}_{i,P}^C + \sum_j \mathcal{M}_{j,P}^A \right\}, \quad (\text{A5})$$

$$\sqrt{2} \mathcal{A}(\overline{B}_d^{*0} \rightarrow D_u^0 \eta_q) = \mathcal{F} V_{cb} V_{ud}^* \left\{ \sum_i \mathcal{M}_{i,P}^C + \sum_j \mathcal{M}_{j,P}^A \right\}, \quad (\text{A6})$$

$$\mathcal{A}(\overline{B}_d^{*0} \rightarrow D_u^0 \overline{K}^0) = \mathcal{F} V_{cb} V_{us}^* \sum_i \mathcal{M}_{i,P}^C, \quad (\text{A7})$$

$$\mathcal{A}(\overline{B}_d^{*0} \rightarrow D_s^+ K^-) = \mathcal{F} V_{cb} V_{ud}^* \sum_i \mathcal{M}_{i,P}^A, \quad (\text{A8})$$

$$\mathcal{A}(\overline{B}_s^{*0} \rightarrow D_s^+ \pi^-) = \mathcal{F} V_{cb} V_{ud}^* \sum_i \mathcal{M}_{i,P}^T, \quad (\text{A9})$$

$$\mathcal{A}(\overline{B}_s^{*0} \rightarrow D_s^+ K^-) = \mathcal{F} V_{cb} V_{us}^* \left\{ \sum_i \mathcal{M}_{i,P}^T + \sum_j \mathcal{M}_{j,P}^A \right\}, \quad (\text{A10})$$

$$\mathcal{A}(\overline{B}_s^{*0} \rightarrow D_d^+ \pi^-) = \mathcal{F} V_{cb} V_{us}^* \sum_i \mathcal{M}_{i,P}^A, \quad (\text{A11})$$

$$\sqrt{2} \mathcal{A}(\overline{B}_s^{*0} \rightarrow D_u^0 \pi^0) = \mathcal{F} V_{cb} V_{us}^* \sum_i \mathcal{M}_{i,P}^A, \quad (\text{A12})$$

$$\sqrt{2} \mathcal{A}(\overline{B}_s^{*0} \rightarrow D_u^0 \eta_q) = \mathcal{F} V_{cb} V_{us}^* \sum_i \mathcal{M}_{i,P}^A, \quad (\text{A13})$$

$$\mathcal{A}(\overline{B}_s^{*0} \rightarrow D_u^0 \eta_s) = \mathcal{F} V_{cb} V_{us}^* \sum_i \mathcal{M}_{i,P}^C, \quad (\text{A14})$$

$$\mathcal{A}(\overline{B}_s^{*0} \rightarrow D_u^0 K^0) = \mathcal{F} V_{cb} V_{ud}^* \sum_i \mathcal{M}_{i,P}^C, \quad (\text{A15})$$

$$\mathcal{F} = \frac{G_F}{\sqrt{2}} \frac{\pi C_F}{N_c} f_{B_q^*} f_D, \quad (\text{A16})$$

where  $\mathcal{M}_{i,j}^k$  is the amplitude building blocks. The superscripts  $k = T, C, A$  correspond to the color-allowed emission topologies of Fig.1, the color-suppressed emission topologies of Fig.2, the annihilation topologies of Fig.3. The subscripts  $i = a, b, c, d$  correspond to the diagram indices. The subscripts  $j = P, L, N, T$  correspond to the different helicity amplitudes. The analytical expressions of the amplitude building blocks  $\mathcal{M}_{i,j}^k$  are given in the Appendix C, D, E.

## Appendix B: The amplitude for the $\overline{B}_q^* \rightarrow DV$ decays

$$i \mathcal{A}_\lambda(B_u^{*-} \rightarrow D_u^0 \rho^-) = \mathcal{F} V_{cb} V_{ud}^* \left\{ \sum_i \mathcal{M}_{i,\lambda}^T + \sum_j \mathcal{M}_{j,\lambda}^C \right\}, \quad (\text{B1})$$

$$i \mathcal{A}_\lambda(B_u^{*-} \rightarrow D_u^0 K^{*-}) = \mathcal{F} V_{cb} V_{us}^* \left\{ \sum_i \mathcal{M}_{i,\lambda}^T + \sum_j \mathcal{M}_{j,\lambda}^C \right\}, \quad (\text{B2})$$

$$i \mathcal{A}_\lambda(\overline{B}_d^{*0} \rightarrow D_d^+ \rho^-) = \mathcal{F} V_{cb} V_{ud}^* \left\{ \sum_i \mathcal{M}_{i,\lambda}^T + \sum_j \mathcal{M}_{j,\lambda}^A \right\}, \quad (\text{B3})$$

$$i \mathcal{A}_\lambda(\overline{B}_d^{*0} \rightarrow D_d^+ K^{*-}) = \mathcal{F} V_{cb} V_{us}^* \sum_i \mathcal{M}_{i,\lambda}^T, \quad (\text{B4})$$

$$i \sqrt{2} \mathcal{A}_\lambda(\overline{B}_d^{*0} \rightarrow D_u^0 \rho^0) = \mathcal{F} V_{cb} V_{ud}^* \left\{ - \sum_i \mathcal{M}_{i,\lambda}^C + \sum_j \mathcal{M}_{j,\lambda}^A \right\}, \quad (\text{B5})$$

$$i \sqrt{2} \mathcal{A}_\lambda(\overline{B}_d^{*0} \rightarrow D_u^0 \omega) = \mathcal{F} V_{cb} V_{ud}^* \left\{ \sum_i \mathcal{M}_{i,\lambda}^C + \sum_j \mathcal{M}_{j,\lambda}^A \right\}, \quad (\text{B6})$$

$$i \mathcal{A}_\lambda(\overline{B}_d^{*0} \rightarrow D_u^0 \overline{K}^{*0}) = \mathcal{F} V_{cb} V_{us}^* \sum_i \mathcal{M}_{i,\lambda}^C, \quad (\text{B7})$$

$$i \mathcal{A}_\lambda(\overline{B}_d^{*0} \rightarrow D_s^+ K^{*-}) = \mathcal{F} V_{cb} V_{ud}^* \sum_i \mathcal{M}_{i,\lambda}^A, \quad (\text{B8})$$

$$i \mathcal{A}_\lambda(\overline{B}_s^{*0} \rightarrow D_s^+ \rho^-) = \mathcal{F} V_{cb} V_{ud}^* \sum_i \mathcal{M}_{i,\lambda}^T, \quad (\text{B9})$$

$$i \mathcal{A}_\lambda(\overline{B}_s^{*0} \rightarrow D_s^+ K^{*-}) = \mathcal{F} V_{cb} V_{us}^* \left\{ \sum_i \mathcal{M}_{i,\lambda}^T + \sum_j \mathcal{M}_{j,\lambda}^A \right\}, \quad (\text{B10})$$

$$i \mathcal{A}_\lambda(\overline{B}_s^{*0} \rightarrow D_d^+ \rho^-) = \mathcal{F} V_{cb} V_{us}^* \sum_i \mathcal{M}_{i,\lambda}^A, \quad (\text{B11})$$

$$i \sqrt{2} \mathcal{A}_\lambda(\overline{B}_s^{*0} \rightarrow D_u^0 \rho^0) = \mathcal{F} V_{cb} V_{us}^* \sum_i \mathcal{M}_{i,\lambda}^A, \quad (\text{B12})$$

$$i \sqrt{2} \mathcal{A}_\lambda(\overline{B}_s^{*0} \rightarrow D_u^0 \omega) = \mathcal{F} V_{cb} V_{us}^* \sum_i \mathcal{M}_{i,\lambda}^A, \quad (\text{B13})$$

$$i \mathcal{A}_\lambda(\overline{B}_s^{*0} \rightarrow D_u^0 \phi) = \mathcal{F} V_{cb} V_{us}^* \sum_i \mathcal{M}_{i,\lambda}^C, \quad (\text{B14})$$

$$i \mathcal{A}_\lambda(\overline{B}_s^{*0} \rightarrow D_u^0 K^{*0}) = \mathcal{F} V_{cb} V_{ud}^* \sum_i \mathcal{M}_{i,\lambda}^C, \quad (\text{B15})$$

where the index  $\lambda$  corresponds to three different helicity amplitudes, i.e.,  $\lambda = L, N, T$ .

### Appendix C: Amplitude building blocks for the color-allowed $\overline{B}_q^* \rightarrow D_q M$ decays

The expressions of the amplitude building blocks  $\mathcal{M}_{i,j}^T$  for the color-allowed topologies are presented as follows, where the subscript  $i$  corresponds to the diagram indices of Fig.1; and  $j$  corresponds to the different helicity amplitudes.

$$\begin{aligned} \mathcal{M}_{a,P}^T &= 2 m_1 p \int_0^1 dx_1 \int_0^1 dx_2 \int_0^\infty b_1 db_1 \int_0^\infty b_2 db_2 H_f^T(\alpha^T, \beta_a^T, b_1, b_2) E_f^T(t_a^T) \\ &\times \alpha_s(t_a^T) a_1(t_a^T) \phi_{B_q^*}^v(x_1) \left\{ \phi_D^a(x_2) (m_1^2 \bar{x}_2 + m_3^2 x_2) + \phi_D^p(x_2) m_2 m_b \right\}, \end{aligned} \quad (\text{C1})$$

$$\begin{aligned}\mathcal{M}_{a,L}^T &= \int_0^1 dx_1 \int_0^1 dx_2 \int_0^\infty b_1 db_1 \int_0^\infty b_2 db_2 H_f^T(\alpha^T, \beta_a^T, b_1, b_2) E_f^T(t_a^T) \alpha_s(t_a^T) \\ &\times a_1(t_a^T) \phi_{B_q^*}^v(x_1) \left\{ \phi_D^a(x_2) (m_1^2 s \bar{x}_2 + m_3^2 t x_2) + \phi_D^p(x_2) m_2 m_b u \right\},\end{aligned}\quad (\text{C2})$$

$$\begin{aligned}\mathcal{M}_{a,N}^T &= m_1 m_3 \int_0^1 dx_1 \int_0^1 dx_2 \int_0^\infty b_1 db_1 \int_0^\infty b_2 db_2 H_f^T(\alpha^T, \beta_a^T, b_1, b_2) E_f^T(t_a^T) \\ &\times \alpha_s(t_a^T) a_1(t_a^T) \phi_{B_q^*}^V(x_1) \left\{ \phi_D^a(x_2) (2 m_2^2 x_2 - t) - 2 m_2 m_b \phi_D^p(x_2) \right\},\end{aligned}\quad (\text{C3})$$

$$\begin{aligned}\mathcal{M}_{a,T}^T &= 2 m_1 m_3 \int_0^1 dx_1 \int_0^1 dx_2 \int_0^\infty b_1 db_1 \int_0^\infty b_2 db_2 H_f^T(\alpha^T, \beta_a^T, b_1, b_2) E_f^T(t_a^T) \\ &\times \alpha_s(t_a^T) a_1(t_a^T) \phi_{B_q^*}^V(x_1) \phi_D^a(x_2),\end{aligned}\quad (\text{C4})$$

$$\begin{aligned}\mathcal{M}_{b,P}^T &= 2 m_1 p \int_0^1 dx_1 \int_0^1 dx_2 \int_0^\infty b_1 db_1 \int_0^\infty b_2 db_2 H_f^T(\alpha^T, \beta_b^T, b_2, b_1) E_f^T(t_b^T) \\ &\times \alpha_s(t_b^T) \left\{ \phi_{B_q^*}^v(x_1) \left[ 2 m_2 m_c \phi_D^p(x_2) - \phi_D^a(x_2) (m_2^2 \bar{x}_1 + m_3^2 x_1) \right] \right. \\ &\left. + \phi_{B_q^*}^t(x_1) \left[ 2 m_1 m_2 \phi_D^p(x_2) \bar{x}_1 - m_1 m_c \phi_D^a(x_2) \right] \right\} a_1(t_b^T),\end{aligned}\quad (\text{C5})$$

$$\begin{aligned}\mathcal{M}_{b,L}^T &= \int_0^1 dx_1 \int_0^1 dx_2 \int_0^\infty b_1 db_1 \int_0^\infty b_2 db_2 H_f^T(\alpha^T, \beta_b^T, b_2, b_1) E_f^T(t_b^T) \alpha_s(t_b^T) \\ &\times a_1(t_b^T) \left\{ \phi_{B_q^*}^t(x_1) \left[ 2 m_1 m_2 \phi_D^p(x_2) (s - u x_1) - m_1 m_c s \phi_D^a(x_2) \right] \right. \\ &\left. + \phi_{B_q^*}^v(x_1) \left[ \phi_D^a(x_2) (m_3^2 t x_1 - m_2^2 u \bar{x}_1) + 2 m_2 m_c u \phi_D^p(x_2) \right] \right\},\end{aligned}\quad (\text{C6})$$

$$\begin{aligned}\mathcal{M}_{b,N}^T &= m_3 \int_0^1 dx_1 \int_0^1 dx_2 \int_0^\infty b_1 db_1 \int_0^\infty b_2 db_2 H_f^T(\alpha^T, \beta_b^T, b_2, b_1) E_f^T(t_b^T) \\ &\times \alpha_s(t_b^T) \left\{ \phi_{B_q^*}^V(x_1) m_1 \left[ \phi_D^a(x_2) (2 m_2^2 - t x_1) - 4 m_2 m_c \phi_D^p(x_2) \right] \right. \\ &\left. + \phi_{B_q^*}^T(x_1) \left[ \phi_D^a(x_2) t m_c + \phi_D^p(x_2) 2 m_2 (2 m_1^2 x_1 - t) \right] \right\} a_1(t_b^T),\end{aligned}\quad (\text{C7})$$

$$\begin{aligned}\mathcal{M}_{b,T}^T &= 2 m_3 \int_0^1 dx_1 \int_0^1 dx_2 \int_0^\infty b_1 db_1 \int_0^\infty b_2 db_2 H_f^T(\alpha^T, \beta_b^T, b_2, b_1) E_f^T(t_b^T) \alpha_s(t_b^T) \\ &\times a_1(t_b^T) \left\{ \phi_{B_q^*}^T(x_1) \left[ \phi_D^p(x_2) 2 m_2 - \phi_D^a(x_2) m_c \right] - \phi_{B_q^*}^V(x_1) \phi_D^a(x_2) m_1 x_1 \right\},\end{aligned}\quad (\text{C8})$$

$$\begin{aligned}\mathcal{M}_{c,P}^T &= \frac{2 m_1 p}{N_c} \int_0^1 dx_1 \int_0^1 dx_2 \int_0^1 dx_3 \int_0^\infty db_1 \int_0^\infty b_2 db_2 \int_0^\infty b_3 db_3 \delta(b_1 - b_2) \\ &\times \phi_P^a(x_3) \alpha_s(t_c^T) C_2(t_c^T) \left\{ \phi_{B_q^*}^v(x_1) \phi_D^a(x_2) (2 m_2^2 x_2 + s \bar{x}_3 - t x_1) \right. \\ &\left. + \phi_{B_q^*}^t(x_1) \phi_D^p(x_2) m_1 m_2 (x_1 - x_2) \right\} H_n^T(\alpha^T, \beta_c^T, b_3, b_2) E_n^T(t_c^T),\end{aligned}\quad (\text{C9})$$

$$\begin{aligned}
\mathcal{M}_{c,L}^T &= \frac{1}{N_c} \int_0^1 dx_1 \int_0^1 dx_2 \int_0^1 dx_3 \int_0^\infty db_1 \int_0^\infty b_2 db_2 \int_0^\infty b_3 db_3 H_n^T(\alpha^T, \beta_c^T, b_3, b_2) \\
&\times \delta(b_1 - b_2) E_n(t_c^T) \phi_V^v(x_3) \left\{ \phi_{B_q^*}^v(x_1) \phi_D^a(x_2) u (2 m_2^2 x_2 + s \bar{x}_3 - t x_1) \right. \\
&+ \left. \phi_{B_q^*}^t(x_1) \phi_D^p(x_2) m_1 m_2 (u x_1 - s x_2 - 2 m_3^2 \bar{x}_3) \right\} \alpha_s(t_c^T) C_2(t_c^T), \tag{C10}
\end{aligned}$$

$$\begin{aligned}
\mathcal{M}_{c,N}^T &= \frac{m_3}{N_c} \int_0^1 dx_1 \int_0^1 dx_2 \int_0^1 dx_3 \int_0^\infty db_1 \int_0^\infty b_2 db_2 \int_0^\infty b_3 db_3 \\
&\times H_n^T(\alpha^T, \beta_c^T, b_3, b_2) E_n(t_c^T) \alpha_s(t_c^T) C_2(t_c^T) \delta(b_1 - b_2) \\
&\times \left\{ \phi_{B_q^*}^V(x_1) \phi_D^a(x_2) \phi_V^V(x_3) 2 m_1 (t x_1 - 2 m_2^2 x_2 - s \bar{x}_3) \right. \\
&+ \phi_{B_q^*}^T(x_1) \phi_D^p(x_2) \phi_V^V(x_3) m_2 (t x_2 + u \bar{x}_3 - 2 m_1^2 x_1) \\
&+ \left. \phi_{B_q^*}^T(x_1) \phi_D^p(x_2) \phi_V^A(x_3) 2 m_1 m_2 p (x_2 - \bar{x}_3) \right\}, \tag{C11}
\end{aligned}$$

$$\begin{aligned}
\mathcal{M}_{c,T}^T &= \frac{m_3}{N_c p} \int_0^1 dx_1 \int_0^1 dx_2 \int_0^1 dx_3 \int_0^\infty db_1 \int_0^\infty b_2 db_2 \int_0^\infty b_3 db_3 \\
&\times H_n^T(\alpha^T, \beta_c^T, b_3, b_2) E_n(t_c^T) \alpha_s(t_c^T) C_2(t_c^T) \delta(b_1 - b_2) \\
&\times \left\{ \phi_{B_q^*}^V(x_1) \phi_D^a(x_2) \phi_V^A(x_3) 2 (2 m_2^2 x_2 + s \bar{x}_3 - t x_1) \right. \\
&+ \phi_{B_q^*}^T(x_1) \phi_D^p(x_2) \phi_V^A(x_3) r_2 (2 m_1^2 x_1 - t x_2 - u \bar{x}_3) \\
&+ \left. \phi_{B_q^*}^T(x_1) \phi_D^p(x_2) \phi_V^V(x_3) 2 m_2 p (\bar{x}_3 - x_2) \right\}, \tag{C12}
\end{aligned}$$

$$\begin{aligned}
\mathcal{M}_{d,P}^T &= \frac{2 m_1 p}{N_c} \int_0^1 dx_1 \int_0^1 dx_2 \int_0^1 dx_3 \int_0^\infty db_1 \int_0^\infty b_2 db_2 \int_0^\infty b_3 db_3 \phi_P^a(x_3) \\
&\times \delta(b_1 - b_2) \alpha_s(t_d^T) C_2(t_d^T) E_n(t_d^T) \left\{ \phi_{B_q^*}^v(x_1) \phi_D^a(x_2) s (x_2 - x_3) \right. \\
&+ \left. \phi_{B_q^*}^t(x_1) \phi_D^p(x_2) m_1 m_2 (x_1 - x_2) \right\} H_n^T(\alpha^T, \beta_d^T, b_3, b_2), \tag{C13}
\end{aligned}$$

$$\begin{aligned}
\mathcal{M}_{d,L}^T &= \frac{1}{N_c} \int_0^1 dx_1 \int_0^1 dx_2 \int_0^1 dx_3 \int_0^\infty db_1 \int_0^\infty b_2 db_2 \int_0^\infty b_3 db_3 \delta(b_1 - b_2) \\
&\times E_n(t_d^T) \alpha_s(t_d^T) C_2(t_d^T) \phi_V^v(x_3) \left\{ \phi_{B_q^*}^v(x_1) \phi_D^a(x_2) 4 m_1^2 p^2 (x_2 - x_3) \right. \\
&+ \left. \phi_{B_q^*}^t(x_1) \phi_D^p(x_2) m_1 m_2 (u x_1 - s x_2 - 2 m_3^2 x_3) \right\} H_n^T(\alpha^T, \beta_d^T, b_3, b_2), \tag{C14}
\end{aligned}$$

$$\begin{aligned}
\mathcal{M}_{d,N}^T &= \frac{m_2 m_3}{N_c} \int_0^1 dx_1 \int_0^1 dx_2 \int_0^1 dx_3 \int_0^\infty db_1 \int_0^\infty b_2 db_2 \int_0^\infty b_3 db_3 \delta(b_1 - b_2) \\
&\times \phi_{B_q^*}^T(x_1) \phi_D^p(x_2) \alpha_s(t_d^T) C_2(t_d^T) \left\{ \phi_V^V(x_3) (t x_2 + u x_3 - 2 m_1^2 x_1) \right. \\
&+ \left. \phi_V^A(x_3) 2 m_1 p (x_2 - x_3) \right\} H_n^T(\alpha^T, \beta_d^T, b_3, b_2) E_n(t_d^T), \tag{C15}
\end{aligned}$$



$$\begin{aligned}
\mathcal{M}_{d,T}^T &= \frac{m_2 m_3}{N_c m_1 p} \int_0^1 dx_1 \int_0^1 dx_2 \int_0^1 dx_3 \int_0^\infty db_1 \int_0^\infty b_2 db_2 \int_0^\infty b_3 db_3 \delta(b_1 - b_2) \\
&\times \phi_{B_q^*}^T(x_1) \phi_D^p(x_2) \alpha_s(t_d^T) C_2(t_d^T) \left\{ \phi_V^A(x_3) (2 m_1^2 x_1 - t x_2 - u x_3) \right. \\
&\left. + \phi_V^V(x_3) 2 m_1 p (x_3 - x_2) \right\} H_n^T(\alpha^T, \beta_d^T, b_3, b_2) E_n(t_d^T), \tag{C16}
\end{aligned}$$

where  $N_c = 3$  is the color number.  $\alpha_s$  is the strong coupling constant.  $C_{1,2}$  are the Wilson coefficients. The parameter  $a_i$  is defined as

$$a_1 = C_1 + \frac{1}{N_c} C_2, \tag{C17}$$

$$a_2 = C_2 + \frac{1}{N_c} C_1. \tag{C18}$$

The functions  $H_{f,n}^T$  and the Sudakov factors  $E_{f,n}^T$  are defined as follows, where the subscripts  $f$  and  $n$  correspond to the factorizable and nonfactorizable topologies.

$$H_f^T(\alpha, \beta, b_i, b_j) = K_0(b_i \sqrt{-\alpha}) \left\{ \theta(b_i - b_j) K_0(b_i \sqrt{-\beta}) I_0(b_j \sqrt{-\beta}) + (b_i \leftrightarrow b_j) \right\}, \tag{C19}$$

$$\begin{aligned}
H_n^T(\alpha, \beta, b_i, b_j) &= \left\{ \theta(b_i - b_j) K_0(b_i \sqrt{-\alpha}) I_0(b_j \sqrt{-\alpha}) + (b_i \leftrightarrow b_j) \right\} \\
&\times \left\{ \theta(-\beta) K_0(b_i \sqrt{-\beta}) + \frac{\pi}{2} \theta(+\beta) \left[ i J_0(b_i \sqrt{\beta}) - Y_0(b_i \sqrt{\beta}) \right] \right\}, \tag{C20}
\end{aligned}$$

$$E_f^T(t) = \exp\{-S_{B_q^*}(t) - S_D(t)\}, \tag{C21}$$

$$E_n(t) = \exp\{-S_{B_q^*}(t) - S_D(t) - S_M(t)\}, \tag{C22}$$

$$S_{B_q^*}(t) = s(x_1, b_1, p_1^+) + 2 \int_{1/b_1}^t \frac{d\mu}{\mu} \gamma_q, \tag{C23}$$

$$S_D(t) = s(x_2, b_2, p_2^+) + s(\bar{x}_2, b_2, p_2^+) + 2 \int_{1/b_2}^t \frac{d\mu}{\mu} \gamma_q, \tag{C24}$$

$$S_M(t) = s(x_3, b_3, p_3^+) + s(\bar{x}_3, b_3, p_3^+) + 2 \int_{1/b_3}^t \frac{d\mu}{\mu} \gamma_q, \tag{C25}$$

where  $I_0$ ,  $J_0$ ,  $K_0$  and  $Y_0$  are the Bessel functions;  $\gamma_q = -\alpha_s/\pi$  is the quark anomalous dimension; the expression of  $s(x, b, Q)$  can be found in the appendix of Ref.[4];  $\alpha^T$  and  $\beta_i^T$  are the virtualities of the gluon and quark propagators; the subscripts of the quark virtuality

$\beta_i^T$  and the typical scale  $t_i^T$  correspond to the diagram indices of Fig.1.

$$\alpha^T = x_1^2 m_1^2 + x_2^2 m_2^2 - x_1 x_2 t, \quad (\text{C26})$$

$$\beta_a^T = x_2^2 m_2^2 - x_2 t + m_1^2 - m_b^2, \quad (\text{C27})$$

$$\beta_b^T = x_1^2 m_1^2 - x_1 t + m_2^2 - m_c^2, \quad (\text{C28})$$

$$\beta_c^T = \alpha^T + \bar{x}_3^2 m_3^2 - x_1 \bar{x}_3 u + x_2 \bar{x}_3 s, \quad (\text{C29})$$

$$\beta_d^T = \alpha^T + x_3^2 m_3^2 - x_1 x_3 u + x_2 x_3 s, \quad (\text{C30})$$

$$t_{a(b)}^T = \max(\sqrt{-\alpha^T}, \sqrt{|\beta_{a(b)}^T|}, 1/b_1, 1/b_2), \quad (\text{C31})$$

$$t_{c(d)}^T = \max(\sqrt{-\alpha^T}, \sqrt{|\beta_{c(d)}^T|}, 1/b_2, 1/b_3). \quad (\text{C32})$$

#### Appendix D: Amplitude building blocks for the color-suppressed $\bar{B}_q^* \rightarrow DM_q$ decays

The expressions of the amplitude building blocks  $\mathcal{M}_{i,j}^C$  for the color-suppressed topologies are displayed as follows, where the subscript  $i$  corresponds to the diagram indices of Fig.2; and  $j$  corresponds to the different helicity amplitudes.

$$\begin{aligned} \mathcal{M}_{a,P}^C = & - \int_0^1 dx_1 \int_0^1 dx_3 \int_0^\infty b_1 db_1 \int_0^\infty b_3 db_3 \phi_{B_q^*}^v(x_1) \alpha_s(t_a^C) a_2(t_a^C) \\ & \times H_f^C(\alpha^C, \beta_a^C, b_1, b_3) \left\{ 2 m_1 p \phi_P^a(x_3) (m_1^2 \bar{x}_3 + m_2^2 x_3) \right. \\ & \left. + 2 m_1 p \mu_P m_b \phi_P^p(x_3) + \mu_P m_b t \phi_P^t(x_3) \right\} E_f^C(t_a^C), \end{aligned} \quad (\text{D1})$$

$$\begin{aligned} \mathcal{M}_{a,L}^C = & - \int_0^1 dx_1 \int_0^1 dx_3 \int_0^\infty b_1 db_1 \int_0^\infty b_3 db_3 H_f^C(\alpha^C, \beta_a^C, b_1, b_3) \\ & \times \alpha_s(t_a^C) a_2(t_a^C) \phi_{B_q^*}^v(x_1) \left\{ \phi_V^v(x_3) (m_1^2 s \bar{x}_3 + m_2^2 u x_3) \right. \\ & \left. + m_3 m_b t \phi_V^t(x_3) + 2 m_1 p m_3 m_b \phi_V^s(x_3) \right\} E_f^C(t_a^C), \end{aligned} \quad (\text{D2})$$

$$\begin{aligned} \mathcal{M}_{a,N}^C = & \int_0^1 dx_1 \int_0^1 dx_3 \int_0^\infty b_1 db_1 \int_0^\infty b_3 db_3 H_f^C(\alpha^C, \beta_a^C, b_1, b_3) \\ & \times \alpha_s(t_a^C) a_2(t_a^C) \phi_{B_q^*}^V(x_1) \left\{ \phi_V^V(x_3) m_1 m_3 (t - s x_3) \right. \\ & \left. + m_1 m_b s \phi_V^T(x_3) + 2 m_3 p m_1^2 \bar{x}_3 \phi_V^A(x_3) \right\} E_f^C(t_a^C), \end{aligned} \quad (\text{D3})$$

$$\begin{aligned} \mathcal{M}_{a,T}^C = & - \int_0^1 dx_1 \int_0^1 dx_3 \int_0^\infty b_1 db_1 \int_0^\infty b_3 db_3 H_f^C(\alpha^C, \beta_a^C, b_1, b_3) \\ & \times \alpha_s(t_a^C) a_2(t_a^C) \phi_{B_q^*}^V(x_1) \left\{ (m_3/p) \phi_V^A(x_3) (t - s x_3) \right. \\ & \left. + \phi_V^V(x_3) 2 m_1 m_3 \bar{x}_3 + \phi_V^T(x_3) 2 m_1 m_b \right\} E_f^C(t_a^C), \end{aligned} \quad (\text{D4})$$

$$\begin{aligned}\mathcal{M}_{b,P}^C &= 2 m_1 p \int_0^1 dx_1 \int_0^1 dx_3 \int_0^\infty b_1 db_1 \int_0^\infty b_3 db_3 H_f^C(\alpha^C, \beta_b^C, b_3, b_1) E_f^C(t_b^C) \alpha_s(t_b^C) \\ &\times a_2(t_b^C) \left\{ \phi_{B_q^*}^v(x_1) \phi_P^a(x_3) (m_3^2 \bar{x}_1 + m_2^2 x_1) - \phi_{B_q^*}^t(x_1) \phi_P^p(x_3) 2 m_1 \mu_P \bar{x}_1 \right\},\end{aligned}\quad (\text{D5})$$

$$\begin{aligned}\mathcal{M}_{b,L}^C &= \int_0^1 dx_1 \int_0^1 dx_3 \int_0^\infty b_1 db_1 \int_0^\infty b_3 db_3 H_f^C(\alpha^C, \beta_b^C, b_3, b_1) E_f^C(t_b^C) \alpha_s(t_b^C) a_2(t_b^C) \\ &\times \left\{ \phi_{B_q^*}^v(x_1) \phi_V^v(x_3) (m_2^2 u x_1 - m_3^2 t \bar{x}_1) - \phi_{B_q^*}^t(x_1) \phi_V^s(x_3) 4 m_1^2 m_3 p \bar{x}_1 \right\},\end{aligned}\quad (\text{D6})$$

$$\begin{aligned}\mathcal{M}_{b,N}^C &= m_1 m_3 \int_0^1 dx_1 \int_0^1 dx_3 \int_0^\infty b_1 db_1 \int_0^\infty b_3 db_3 H_f^C(\alpha^C, \beta_b^C, b_3, b_1) E_f^C(t_b^C) \\ &\times \alpha_s(t_b^C) a_2(t_b^C) \phi_{B_q^*}^V(x_1) \left\{ \phi_V^V(x_3) (s - t x_1) + \phi_V^A(x_3) 2 m_1 p \bar{x}_1 \right\},\end{aligned}\quad (\text{D7})$$

$$\begin{aligned}\mathcal{M}_{b,T}^C &= \frac{-m_3}{p} \int_0^1 dx_1 \int_0^1 dx_3 \int_0^\infty b_1 db_1 \int_0^\infty b_3 db_3 H_f^C(\alpha^C, \beta_b^C, b_3, b_1) E_f^C(t_b^C) \\ &\times \alpha_s(t_b^C) a_2(t_b^C) \phi_{B_q^*}^V(x_1) \left\{ \phi_V^A(x_3) (s - t x_1) + \phi_V^V(x_3) 2 m_1 p \bar{x}_1 \right\},\end{aligned}\quad (\text{D8})$$

$$\begin{aligned}\mathcal{M}_{c,P}^C &= \int_0^1 dx_1 \int_0^1 dx_2 \int_0^1 dx_3 \int_0^\infty db_1 \int_0^\infty b_2 db_2 \int_0^\infty b_3 db_3 H_n^C(\alpha^C, \beta_c^C, b_2, b_3) \\ &\times \delta(b_1 - b_3) \left\{ \phi_{B_q^*}^t(x_1) \phi_D^a(x_2) m_1 \mu_P \left[ \phi_P^t(x_3) (t x_1 - 2 m_2^2 \bar{x}_2 - s x_3) \right. \right. \\ &+ \left. \phi_P^p(x_3) 2 m_1 p (x_3 - x_1) \right] - \phi_{B_q^*}^v(x_1) \phi_P^a(x_3) 2 m_1 p \left[ \phi_D^p(x_2) m_2 m_c \right. \\ &+ \left. \phi_D^a(x_2) (s \bar{x}_2 + 2 m_3^2 x_3 - u x_1) \right] \left. \right\} E_n(t_c^C) \alpha_s(t_c^C) C_1(t_c^C)/N_c,\end{aligned}\quad (\text{D9})$$

$$\begin{aligned}\mathcal{M}_{c,L}^C &= \int_0^1 dx_1 \int_0^1 dx_2 \int_0^1 dx_3 \int_0^\infty db_1 \int_0^\infty b_2 db_2 \int_0^\infty b_3 db_3 H_n^C(\alpha^C, \beta_c^C, b_2, b_3) \\ &\times \delta(b_1 - b_3) \left\{ \phi_{B_q^*}^t(x_1) \phi_D^a(x_2) m_1 m_3 \left[ \phi_V^t(x_3) (t x_1 - 2 m_2^2 \bar{x}_2 - s x_3) \right. \right. \\ &+ \left. \phi_V^s(x_3) 2 m_1 p (x_3 - x_1) \right] + \phi_{B_q^*}^v(x_1) \phi_V^v(x_3) \left[ - \phi_D^p(x_2) m_2 m_c u \right. \\ &+ \left. \phi_D^a(x_2) 4 m_1^2 p^2 (x_1 - \bar{x}_2) \right] \left. \right\} E_n(t_c^C) \alpha_s(t_c^C) C_1(t_c^C)/N_c,\end{aligned}\quad (\text{D10})$$

$$\begin{aligned}\mathcal{M}_{c,N}^C &= \frac{1}{N_c} \int_0^1 dx_1 \int_0^1 dx_2 \int_0^1 dx_3 \int_0^\infty db_1 \int_0^\infty b_2 db_2 \int_0^\infty b_3 db_3 H_n^C(\alpha^C, \beta_c^C, b_2, b_3) \\ &\times \delta(b_1 - b_3) E_n(t_c^C) \alpha_s(t_c^C) \left\{ \phi_{B_q^*}^V(x_1) \phi_D^p(x_2) \phi_V^V(x_3) 2 m_1 m_2 m_3 m_c \right. \\ &+ \left. \phi_{B_q^*}^T(x_1) \phi_D^a(x_2) \phi_V^T(x_3) \left[ m_1^2 s (\bar{x}_2 - x_1) + m_3^2 t (x_3 - \bar{x}_2) \right] \right\} C_1(t_c^C),\end{aligned}\quad (\text{D11})$$

$$\begin{aligned}
\mathcal{M}_{c,T}^C &= \frac{2}{N_c} \int_0^1 dx_1 \int_0^1 dx_2 \int_0^1 dx_3 \int_0^\infty db_1 \int_0^\infty b_2 db_2 \int_0^\infty b_3 db_3 H_n^C(\alpha^C, \beta_c^C, b_2, b_3) \\
&\times C_1(t_c^C) \left\{ \phi_{B_q^*}^T(x_1) \phi_D^a(x_2) \phi_V^T(x_3) \left[ m_1^2 (x_1 - \bar{x}_2) + m_3^2 (\bar{x}_2 - x_3) \right] \right. \\
&\left. - \phi_{B_q^*}^V(x_1) \phi_D^p(x_2) \phi_V^A(x_3) m_2 m_3 m_c/p \right\} E_n(t_c^C) \alpha_s(t_c^C) \delta(b_1 - b_3), \tag{D12}
\end{aligned}$$

$$\begin{aligned}
\mathcal{M}_{d,P}^C &= \frac{1}{N_c} \int_0^1 dx_1 \int_0^1 dx_2 \int_0^1 dx_3 \int_0^\infty db_1 \int_0^\infty b_2 db_2 \int_0^\infty b_3 db_3 H_n^C(\alpha^C, \beta_d^C, b_2, b_3) E_n(t_d^C) \\
&\times \delta(b_1 - b_3) \alpha_s(t_d^C) C_1(t_d^C) \phi_D^a(x_2) \left\{ \phi_{B_q^*}^v(x_1) \phi_P^a(x_3) 2 m_1 p s (x_2 - x_3) \right. \\
&\left. + \phi_{B_q^*}^t(x_1) m_1 \mu_P \left[ \phi_P^p(x_3) 2 m_1 p (x_3 - x_1) + \phi_P^t(x_3) (2 m_2^2 x_2 + s x_3 - t x_1) \right] \right\} \tag{D13}
\end{aligned}$$

$$\begin{aligned}
\mathcal{M}_{d,L}^C &= \frac{1}{N_c} \int_0^1 dx_1 \int_0^1 dx_2 \int_0^1 dx_3 \int_0^\infty db_1 \int_0^\infty b_2 db_2 \int_0^\infty b_3 db_3 H_n^C(\alpha^C, \beta_d^C, b_2, b_3) E_n(t_d^C) \\
&\times \delta(b_1 - b_3) \alpha_s(t_d^C) C_1(t_d^C) \phi_D^a(x_2) \left\{ \phi_{B_q^*}^v(x_1) \phi_V^v(x_3) 4 m_1^2 p^2 (x_2 - x_3) \right. \\
&\left. + \phi_{B_q^*}^t(x_1) m_1 m_3 \left[ \phi_V^s(x_3) 2 m_1 p (x_3 - x_1) + \phi_V^t(x_3) (2 m_2^2 x_2 + s x_3 - t x_1) \right] \right\} \tag{D14}
\end{aligned}$$

$$\begin{aligned}
\mathcal{M}_{d,N}^C &= \frac{1}{N_c} \int_0^1 dx_1 \int_0^1 dx_2 \int_0^1 dx_3 \int_0^\infty db_1 \int_0^\infty b_2 db_2 \int_0^\infty b_3 db_3 H_n^C(\alpha^C, \beta_d^C, b_2, b_3) E_n(t_d^C) \\
&\times \delta(b_1 - b_3) \alpha_s(t_d^C) C_1(t_d^C) \phi_{B_q^*}^T(x_1) \phi_D^a(x_2) \phi_V^T(x_3) \left\{ m_1^2 s (x_1 - x_2) + m_3^2 t (x_2 - x_3) \right\} \tag{D15}
\end{aligned}$$

$$\begin{aligned}
\mathcal{M}_{d,T}^C &= \frac{2}{N_c} \int_0^1 dx_1 \int_0^1 dx_2 \int_0^1 dx_3 \int_0^\infty db_1 \int_0^\infty b_2 db_2 \int_0^\infty b_3 db_3 H_n^C(\alpha^C, \beta_d^C, b_2, b_3) E_n(t_d^C) \\
&\times \delta(b_1 - b_3) \alpha_s(t_d^C) C_1(t_d^C) \phi_{B_q^*}^T(x_1) \phi_D^a(x_2) \phi_V^T(x_3) \left\{ m_1^2 (x_2 - x_1) + m_3^2 (x_3 - x_2) \right\} \tag{D16}
\end{aligned}$$

The functions  $H_{f,n}^C$  have the similar expressions for  $H_{f,n}^T$ , i.e.,

$$H_f^C(\alpha, \beta, b_i, b_j) = H_f^T(\alpha, \beta, b_i, b_j), \tag{D17}$$

$$H_n^C(\alpha, \beta, b_i, b_j) = H_n^T(\alpha, \beta, b_i, b_j). \tag{D18}$$

The Sudakov factor  $E_f^C$  are defined as

$$E_f^C(t) = \exp\{-S_{B_q^*}(t) - S_M(t)\}, \tag{D19}$$

and the expressions for  $E_n(t)$ ,  $S_{B_q^*}(t)$ ,  $S_D(t)$  and  $S_M(t)$  are the same as those given in the Appendix C.  $\alpha^C$  and  $\beta_i^C$  are the gluon and quark virtualities; the subscripts of  $\beta_i^C$  and  $t_i^C$

correspond to the diagram indices of Fig.2.

$$\alpha^C = x_1^2 m_1^2 + x_3^2 m_3^2 - x_1 x_3 u, \quad (\text{D20})$$

$$\beta_a^C = x_3^2 m_3^2 - x_3 u + m_1^2 - m_b^2, \quad (\text{D21})$$

$$\beta_b^C = x_1^2 m_1^2 - x_1 u + m_3^2, \quad (\text{D22})$$

$$\beta_c^C = \alpha^C + \bar{x}_2^2 m_2^2 - x_1 \bar{x}_2 t + x_3 \bar{x}_2 s - m_c^2, \quad (\text{D23})$$

$$\beta_d^C = \alpha^C + x_2^2 m_2^2 - x_1 x_2 t + x_2 x_3 s, \quad (\text{D24})$$

$$t_{a(b)}^C = \max(\sqrt{-\alpha^C}, \sqrt{|\beta_{a(b)}^C|}, 1/b_1, 1/b_3), \quad (\text{D25})$$

$$t_{c(d)}^C = \max(\sqrt{-\alpha^C}, \sqrt{|\beta_{c(d)}^C|}, 1/b_2, 1/b_3). \quad (\text{D26})$$

### Appendix E: Amplitude building blocks for the annihilation $\bar{B}^{*0} \rightarrow DM$ decays

The expressions of the amplitude building blocks  $\mathcal{M}_{i,j}^A$  for the annihilation topologies are listed as follows, where the subscript  $i$  corresponds to the diagram indices of Fig.3; and  $j$  corresponds to different helicity amplitudes.

$$\begin{aligned} \mathcal{M}_{a,P}^A = & \int_0^1 dx_2 \int_0^1 dx_3 \int_0^\infty b_2 db_2 \int_0^\infty b_3 db_3 H_f^A(\alpha^A, \beta_a^A, b_2, b_3) E_f^A(t_a^A) \alpha_s(t_a^A) \\ & \times a_2(t_a^A) \left\{ \phi_D^p(x_2) \left[ \phi_P^a(x_3) 4 m_1 m_2 m_c p + \phi_P^p(x_3) 4 m_1 m_2 \mu_P p x_3 \right. \right. \\ & + \left. \phi_P^t(x_3) 2 m_2 \mu_P (t + u \bar{x}_3) \right] - \phi_D^a(x_2) \left[ \phi_P^p(x_3) 2 m_1 m_c \mu_P p \right. \\ & + \left. \left. \phi_P^a(x_3) 2 m_1 p (m_1^2 \bar{x}_3 + m_2^2 x_3) + \phi_P^t(x_3) m_c \mu_P t \right] \right\}, \end{aligned} \quad (\text{E1})$$

$$\begin{aligned} \mathcal{M}_{a,L}^A = & \int_0^1 dx_2 \int_0^1 dx_3 \int_0^\infty b_2 db_2 \int_0^\infty b_3 db_3 H_f^A(\alpha^A, \beta_a^A, b_2, b_3) E_f^A(t_a^A) \alpha_s(t_a^A) \\ & \times a_2(t_a^A) \left\{ \phi_D^p(x_2) \left[ \phi_V^v(x_3) 2 m_2 m_c u - \phi_V^t(x_3) 2 m_2 m_3 (t + u \bar{x}_3) \right. \right. \\ & - \left. \left. \phi_V^s(x_3) 4 m_1 m_2 m_3 p x_3 \right] + \phi_D^a(x_2) \left[ \phi_V^s(x_3) 2 m_1 m_3 m_c p \right. \right. \\ & - \left. \left. \phi_V^v(x_3) (m_2^2 u x_3 + m_1^2 s \bar{x}_3) + \phi_V^t(x_3) m_3 m_c t \right] \right\}, \end{aligned} \quad (\text{E2})$$

$$\begin{aligned} \mathcal{M}_{a,N}^A = & \int_0^1 dx_2 \int_0^1 dx_3 \int_0^\infty b_2 db_2 \int_0^\infty b_3 db_3 H_f^A(\alpha^A, \beta_a^A, b_2, b_3) E_f^A(t_a^A) \\ & \times \left\{ \phi_D^a(x_2) \left[ \phi_V^v(x_3) m_1 m_3 (s \bar{x}_3 + 2 m_2^2) - \phi_V^T(x_3) m_1 m_c s \right. \right. \\ & + \left. \left. \phi_V^A(x_3) 2 m_1^2 m_3 p \bar{x}_3 \right] - \phi_D^p(x_2) \left[ \phi_V^v(x_3) 4 m_1 m_2 m_3 m_c \right. \right. \\ & - \left. \left. \phi_V^T(x_3) 2 m_1 m_2 (s + 2 m_3^2 \bar{x}_3) \right] \right\} \alpha_s(t_a^A) a_2(t_a^A), \end{aligned} \quad (\text{E3})$$

$$\begin{aligned}
\mathcal{M}_{a,T}^A = & \int_0^1 dx_2 \int_0^1 dx_3 \int_0^\infty b_2 db_2 \int_0^\infty b_3 db_3 H_f^A(\alpha^A, \beta_a^A, b_2, b_3) E_f^A(t_a^A) \\
& \times \left\{ \phi_D^p(x_2) 4 m_2 \left[ \phi_V^T(x_3) m_1 + \phi_V^A(x_3) m_3 m_c/p \right] \right. \\
& - \phi_D^a(x_2) \left[ \phi_V^V(x_3) 2 m_1 m_3 \bar{x}_3 + \phi_V^T(x_3) 2 m_1 m_c \right. \\
& \left. \left. + \phi_V^A(x_3) (m_3/p) (s \bar{x}_3 + 2 m_2^2) \right] \right\} \alpha_s(t_a^A) a_2(t_a^A), \tag{E4}
\end{aligned}$$

$$\begin{aligned}
\mathcal{M}_{b,P}^A = & 2 m_1 p \int_0^1 dx_2 \int_0^1 dx_3 \int_0^\infty b_2 db_2 \int_0^\infty b_3 db_3 H_f^A(\alpha^A, \beta_b^A, b_3, b_2) E_f^A(t_b^A) \alpha_s(t_b^A) \\
& \times a_2(t_b^A) \left\{ \phi_D^p(x_2) \phi_P^p(x_3) 2 m_2 \mu_P \bar{x}_2 - \phi_D^a(x_2) \phi_P^a(x_3) (m_1^2 x_2 + m_3^2 \bar{x}_2) \right\}, \tag{E5}
\end{aligned}$$

$$\begin{aligned}
\mathcal{M}_{b,L}^A = & - \int_0^1 dx_2 \int_0^1 dx_3 \int_0^\infty b_2 db_2 \int_0^\infty b_3 db_3 H_f^A(\alpha^A, \beta_b^A, b_3, b_2) E_f^A(t_b^A) \alpha_s(t_b^A) a_2(t_b^A) \\
& \times \left\{ \phi_D^p(x_2) \phi_V^s(x_3) 4 m_1 m_2 m_3 p \bar{x}_2 + \phi_D^a(x_2) \phi_V^v(x_3) (m_1^2 s x_2 + m_3^2 t \bar{x}_2) \right\}, \tag{E6}
\end{aligned}$$

$$\begin{aligned}
\mathcal{M}_{b,N}^A = & m_1 m_3 \int_0^1 dx_2 \int_0^1 dx_3 \int_0^\infty b_2 db_2 \int_0^\infty b_3 db_3 H_f^A(\alpha^A, \beta_b^A, b_3, b_2) E_f^A(t_b^A) \\
& \times \alpha_s(t_b^A) a_2(t_b^A) \phi_D^a(x_2) \left\{ \phi_V^V(x_3) (s + 2 m_2^2 x_2) - \phi_V^A(x_3) 2 m_1 p \right\}, \tag{E7}
\end{aligned}$$

$$\begin{aligned}
\mathcal{M}_{b,T}^A = & \int_0^1 dx_2 \int_0^1 dx_3 \int_0^\infty b_2 db_2 \int_0^\infty b_3 db_3 H_f^A(\alpha^A, \beta_b^A, b_3, b_2) E_f^A(t_b^A) \alpha_s(t_b^A) \\
& \times a_2(t_b^A) \phi_D^a(x_2) \left\{ \phi_V^V(x_3) 2 m_1 m_3 - \phi_V^A(x_3) (m_3/p) (s + 2 m_2^2 x_2) \right\}, \tag{E8}
\end{aligned}$$

$$\begin{aligned}
\mathcal{M}_{c,P}^A = & \int_0^1 dx_1 \int_0^1 dx_2 \int_0^1 dx_3 \int_0^\infty b_1 db_1 \int_0^\infty b_2 db_2 \int_0^\infty db_3 H_n^A(\alpha^A, \beta_c^A, b_1, b_2) \\
& \times \delta(b_2 - b_3) \left\{ \phi_D^a(x_2) \phi_P^a(x_3) 2 m_1 p \left[ \phi_{B_q^*}^v(x_1) (s x_2 + 2 m_3^2 \bar{x}_3 - u \bar{x}_1) \right. \right. \\
& + \left. \phi_{B_q^*}^t(x_1) m_1 m_b \right] + \phi_{B_q^*}^v(x_1) \phi_D^p(x_2) m_2 \mu_p \left[ \phi_P^p(x_3) 2 m_1 p (x_2 - \bar{x}_3) \right. \\
& \left. \left. + \phi_P^t(x_3) (2 m_1^2 \bar{x}_1 - t x_2 - u \bar{x}_3) \right] \right\} E_n(t_c^A) \alpha_s(t_c^A) C_1(t_c^A)/N_c, \tag{E9}
\end{aligned}$$

$$\begin{aligned}
\mathcal{M}_{c,L}^A = & \int_0^1 dx_1 \int_0^1 dx_2 \int_0^1 dx_3 \int_0^\infty b_1 db_1 \int_0^\infty b_2 db_2 \int_0^\infty db_3 H_n^A(\alpha^A, \beta_c^A, b_1, b_2) \\
& \times \delta(b_2 - b_3) \left\{ \phi_{B_q^*}^v(x_1) \phi_D^p(x_2) m_2 m_3 \left[ \phi_V^t(x_3) (t x_2 + u \bar{x}_3 - 2 m_1^2 \bar{x}_1) \right. \right. \\
& + \left. \phi_V^s(x_3) 2 m_1 p (\bar{x}_3 - x_2) \right] + \phi_D^a(x_2) \phi_V^v(x_3) \left[ \phi_{B_q^*}^t(x_1) m_1 m_b s \right. \\
& \left. \left. + \phi_{B_q^*}^v(x_1) 4 m_1^2 p^2 (x_2 - \bar{x}_1) \right] \right\} E_n(t_c^A) \alpha_s(t_c^A) C_1(t_c^A)/N_c, \tag{E10}
\end{aligned}$$

$$\begin{aligned}
\mathcal{M}_{c,N}^A &= \int_0^1 dx_1 \int_0^1 dx_2 \int_0^1 dx_3 \int_0^\infty b_1 db_1 \int_0^\infty b_2 db_2 \int_0^\infty db_3 H_n^A(\alpha^A, \beta_c^A, b_1, b_2) E_n(t_c^A) \\
&\times \delta(b_2 - b_3) \alpha_s(t_c^A) \left\{ \phi_{B_q^*}^V(x_1) \phi_D^p(x_2) \phi_V^T(x_3) m_1 m_2 (u \bar{x}_1 - s x_2 - 2 m_3^2 \bar{x}_3) \right. \\
&+ \left. \phi_{B_q^*}^T(x_1) \phi_D^a(x_2) m_3 m_b \left[ \phi_V^A(x_3) 2 m_1 p - \phi_V^V(x_3) t \right] \right\} C_1(t_c^A)/N_c, \quad (E11)
\end{aligned}$$

$$\begin{aligned}
\mathcal{M}_{c,T}^A &= \int_0^1 dx_1 \int_0^1 dx_2 \int_0^1 dx_3 \int_0^\infty b_1 db_1 \int_0^\infty b_2 db_2 \int_0^\infty db_3 H_n^A(\alpha^A, \beta_c^A, b_1, b_2) \\
&\times \delta(b_2 - b_3) E_n(t_c^A) \alpha_s(t_c^A) \left\{ \phi_{B_q^*}^V(x_1) \phi_D^p(x_2) \phi_V^T(x_3) 2 m_1 m_2 (\bar{x}_1 - x_2) \right. \\
&+ \left. \phi_{B_q^*}^T(x_1) \phi_D^a(x_2) m_3 m_b \left[ \phi_V^A(x_3) t/(m_1 p) - 2 \phi_V^V(x_3) \right] \right\} C_1(t_c^A)/N_c, \quad (E12)
\end{aligned}$$

$$\begin{aligned}
\mathcal{M}_{d,P}^A &= \frac{1}{N_c} \int_0^1 dx_1 \int_0^1 dx_2 \int_0^1 dx_3 \int_0^\infty b_1 db_1 \int_0^\infty b_2 db_2 \int_0^\infty db_3 H_n^A(\alpha^A, \beta_d^A, b_1, b_2) E_n(t_d^A) \\
&\times \delta(b_2 - b_3) \alpha_s(t_d^A) C_1(t_d^A) \phi_{B_q^*}^v(x_1) \left\{ \phi_D^a(x_2) \phi_P^a(x_3) 2 m_1 p (2 m_2^2 x_2 + s \bar{x}_3 - t x_1) \right. \\
&+ \left. \phi_D^p(x_2) m_2 \mu_P \left[ \phi_P^t(x_3) (2 m_1^2 x_1 - t x_2 - u \bar{x}_3) + \phi_P^p(x_3) 2 m_1 p (\bar{x}_3 - x_2) \right] \right\}, \quad (E13)
\end{aligned}$$

$$\begin{aligned}
\mathcal{M}_{d,L}^A &= \frac{1}{N_c} \int_0^1 dx_1 \int_0^1 dx_2 \int_0^1 dx_3 \int_0^\infty b_1 db_1 \int_0^\infty b_2 db_2 \int_0^\infty db_3 H_n^A(\alpha^A, \beta_d^A, b_1, b_2) E_n(t_d^A) \\
&\times \delta(b_2 - b_3) \alpha_s(t_d^A) C_1(t_d^A) \phi_{B_q^*}^v(x_1) \left\{ \phi_D^a(x_2) \phi_V^v(x_3) u (2 m_2^2 x_2 + s \bar{x}_3 - t x_1) \right. \\
&- \left. \phi_D^p(x_2) m_2 m_3 \left[ \phi_V^t(x_3) (2 m_1^2 x_1 - t x_2 - u \bar{x}_3) + \phi_V^s(x_3) 2 m_1 p (\bar{x}_3 - x_2) \right] \right\} \quad (E14)
\end{aligned}$$

$$\begin{aligned}
\mathcal{M}_{d,N}^A &= \frac{1}{N_c} \int_0^1 dx_1 \int_0^1 dx_2 \int_0^1 dx_3 \int_0^\infty b_1 db_1 \int_0^\infty b_2 db_2 \int_0^\infty db_3 H_n^A(\alpha^A, \beta_d^A, b_1, b_2) \\
&\times E_n(t_d^A) \alpha_s(t_d^A) \phi_{B_q^*}^V(x_1) \left\{ \phi_D^a(x_2) \phi_V^V(x_3) 2 m_1 m_3 (t x_1 - 2 m_2^2 x_2 - s \bar{x}_3) \right. \\
&+ \left. \phi_D^p(x_2) \phi_V^T(x_3) m_1 m_2 (u x_1 - s x_2 - 2 m_3^2 \bar{x}_3) \right\} C_1(t_d^A) \delta(b_2 - b_3), \quad (E15)
\end{aligned}$$

$$\begin{aligned}
\mathcal{M}_{d,T}^A &= \frac{2}{N_c} \int_0^1 dx_1 \int_0^1 dx_2 \int_0^1 dx_3 \int_0^\infty b_1 db_1 \int_0^\infty b_2 db_2 \int_0^\infty db_3 H_n^A(\alpha^A, \beta_d^A, b_1, b_2) \\
&\times E_n(t_d^A) \alpha_s(t_d^A) \phi_{B_q^*}^V(x_1) \left\{ \phi_D^a(x_2) \phi_V^A(x_3) (m_3/p) (2 m_2^2 x_2 + s \bar{x}_3 - t x_1) \right. \\
&+ \left. \phi_D^p(x_2) \phi_V^T(x_3) m_1 m_2 (x_1 - x_2) \right\} C_1(t_d^A) \delta(b_2 - b_3). \quad (E16)
\end{aligned}$$

The functions  $H_{f,n}^A$  and the Sudakov factor  $E_f^A$  are defined as follows.

$$\begin{aligned}
H_f^A(\alpha, \beta, b_i, b_j) &= \frac{\pi^2}{4} \left\{ i J_0(b_i \sqrt{\alpha}) - Y_0(b_i \sqrt{\alpha}) \right\} \\
&\times \left\{ \theta(b_i - b_j) \left[ i J_0(b_i \sqrt{\beta}) - Y_0(b_i \sqrt{\beta}) \right] J_0(b_j \sqrt{\beta}) + (b_i \leftrightarrow b_j) \right\}, \quad (E17)
\end{aligned}$$

$$H_n^A(\alpha, \beta, b_i, b_j) = \left\{ \theta(-\beta) K_0(b_i \sqrt{-\beta}) + \frac{\pi}{2} \theta(+\beta) \left[ i J_0(b_i \sqrt{\beta}) - Y_0(b_i \sqrt{\beta}) \right] \right\} \\ \times \frac{\pi}{2} \left\{ \theta(b_i - b_j) \left[ i J_0(b_i \sqrt{\alpha}) - Y_0(b_i \sqrt{\alpha}) \right] J_0(b_j \sqrt{\alpha}) + (b_i \leftrightarrow b_j) \right\}, \quad (\text{E18})$$

$$E_f^A(t) = \exp\{-S_D(t) - S_M(t)\}, \quad (\text{E19})$$

and the expressions for  $E_n(t)$ ,  $S_{B_q^*}(t)$ ,  $S_D(t)$  and  $S_M(t)$  are the same as those given in the Appendix C.  $\alpha^A$  and  $\beta_i^A$  are the gluon and quark virtualities; the subscripts of  $\beta_i^A$  and  $t_i^A$  correspond to the diagram indices of Fig.3.

$$\alpha^A = x_2^2 m_2^2 + \bar{x}_3^2 m_3^2 + x_2 \bar{x}_3 s, \quad (\text{E20})$$

$$\beta_a^A = \bar{x}_3^2 m_3^2 + \bar{x}_3 s + m_2^2 - m_c^2, \quad (\text{E21})$$

$$\beta_b^A = x_2^2 m_2^2 + x_2 s + m_3^2, \quad (\text{E22})$$

$$\beta_c^A = \alpha^A + \bar{x}_1^2 m_1^2 - \bar{x}_1 x_2 t - \bar{x}_1 \bar{x}_3 u - m_b^2, \quad (\text{E23})$$

$$\beta_d^A = \alpha^A + x_1^2 m_1^2 - x_1 x_2 t - x_1 \bar{x}_3 u, \quad (\text{E24})$$

$$t_{a(b)}^A = \max(\sqrt{\alpha^A}, \sqrt{|\beta_{a(b)}^A|}, 1/b_2, 1/b_3), \quad (\text{E25})$$

$$t_{c(d)}^A = \max(\sqrt{\alpha^A}, \sqrt{|\beta_{c(d)}^A|}, 1/b_1, 1/b_2). \quad (\text{E26})$$

- 
- [1] C. Patrignani *et al.* (Particle Data Group), Chin. Phys. C 40, 100001 (2016).
  - [2] Ed. A. Bevan *et al.*, Eur. Phys. J. C 74, 3026 (2014).
  - [3] <http://lhcb-operationsplots.web.cern.ch/lhcb-operationsplots/index.htm>.
  - [4] H. Li, Phys. Rev. D 52, 3958 (1995).
  - [5] C. Chang, H. Li, Phys. Rev. D 55, 5577 (1997).
  - [6] T. Yeh, H. Li, Phys. Rev. D 56, 1615 (1997).
  - [7] Y. Keum, H. Li, A. Sanda, Phys. Lett. B 504, 6 (2001).
  - [8] Y. Keum, H. Li, A. Sanda, Phys. Rev. D 63, 054008 (2001).
  - [9] Y. Keum, H. Li, Phys. Rev. D 63, 074006 (2001).
  - [10] C. Lü, K. Ukai, M. Yang, Phys. Rev. D 63, 074009 (2001).
  - [11] C. Lü, M. Yang, Eur. Phys. J. C 23, 275 (2002).
  - [12] M. Beneke *et al.*, Phys. Rev. Lett. 83, 1914 (1999).



- [13] M. Beneke *et al.*, Nucl. Phys. B 591, 313 (2000).
- [14] M. Beneke *et al.*, Nucl. Phys. B 606, 245 (2001).
- [15] D. Du, D. Yang, G. Zhu, Phys. Lett. B 488, 46 (2000).
- [16] D. Du, D. Yang, G. Zhu, Phys. Lett. B 509, 263 (2001).
- [17] D. Du, D. Yang, G. Zhu, Phys. Rev. D 64, 014036 (2001).
- [18] M. Beneke, J. Rohrer, D. Yang, Nucl. Phys. B 774, 64 (2007).
- [19] J. Sun *et al.*, Phys. Rev. D 77, 074013 (2008).
- [20] C. Bauer, S. Fleming, M. Luke, Phys. Rev. D 63, 014006 (2000).
- [21] C. Bauer *et al.*, Phys. Rev. D 63, 114020 (2001).
- [22] C. Bauer, I. Stewart, Phys. Lett. B 516, 134 (2001).
- [23] C. Bauer, D. Pirjol, I. Stewart, Phys. Rev. D 65, 054022 (2002).
- [24] C. Bauer *et al.*, Phys. Rev. D 66, 014017 (2002).
- [25] M. Beneke *et al.*, Nucl. Phys. B 643, 431 (2002).
- [26] M. Beneke, T. Feldmann, Phys. Lett. B 553, 267 (2003).
- [27] M. Beneke, T. Feldmann, Nucl. Phys. B 685, 249 (2004).
- [28] J. Chay, Phys. Lett. B 476, 339 (2000).
- [29] Y. Keum *et al.*, Phys. Rev. D 69, 094018 (2004).
- [30] R. Li, C. Lü, H. Zou, Phys. Rev. D 78, 014018 (2008).
- [31] Q. Chang *et al.*, Eur. Phys. J. C 76, 523 (2016).
- [32] V. Šimonis, Eur. Phys. J. A 52, 90 (2016).
- [33] G. Buchalla, A. Buras, M. Lautenbacher, Rev. Mod. Phys. 68, 1125, (1996).
- [34] J. Bjorken, Nucl. Phys. B (Proc. Suppl.) 11, 325 (1989).
- [35] G. Lepage, S. Brodsky, Phys. Rev. D 22, 2157 (1980).
- [36] P. Ball *et al.*, Nucl. Phys. B 529, 323 (1998).
- [37] T. Kurimoto, H. Li, A. Sanda, Phys. Rev. D 65, 014007 (2001).
- [38] J. Sun *et al.*, Phys. Rev. D 92, 074028 (2015).
- [39] Y. Yang *et al.*, Phys. Lett. B 751, 171 (2015).
- [40] J. Sun *et al.*, Phys. Lett. B 752, 322 (2016).
- [41] P. Ball, JHEP, 9901, 010 (1999).
- [42] P. Ball, G. Jones, JHEP, 0703, 069 (2007).
- [43] P. Ball, V. Braun, A. Lenz, JHEP, 0605, 004 (2006).

- [44] C. Chen, Y. Keum, H. Li, Phys. Rev. D 66, 054013 (2002).
- [45] Y. Yang *et al.*, Int. J. Mod. Phys. A 31, 1650146 (2016).
- [46] J. Sun *et al.*, Nucl. Phys. B 911, 890 (2016).
- [47] J. Sun *et al.*, Phys. Rev. D 95, 036024 (2017).
- [48] Th. Feldmann, P. Kroll and B. Stech, Phys. Rev. D 58, 114006 (1998).
- [49] C. Cheung, C. Hwang, JHEP, 1404, 177 (2014).
- [50] A. Kamal, Particle Physics, Springer-Verlag Berlin Heidelberg, 2014, p. 297-298.
- [51] B. Colquhoun *et al.* (HPQCD Collaboration), Phys. Rev. D 91, 114509 (2015).
- [52] Ed. A. Bevan *et al.*, Eur. Phys. J. C 74, 3026 (2014).
- [53] T. Gershon, M. Needham, Comptes Rendus Physique 16, 435 (2015).
- [54] R. Aaij . *et al.* (LHCb Collaboration), Phys. Rev. Lett. 118, 052002 (2017).
- [55] A. Akeroyd *et al.*, arXiv:1002.5012[hep-ex].